seeking a consensus.
Arch Pathol Lab Med 110 : 997-1005, 1986

5) Ishii N, Hiraga H, Sawamura Y, Shinohe Y, Nagashima K : Alternative EWS-FLI1 fusion gene and MIC2 expression in peripheral and central primitive neuroectodermal tumors. Neuropathology 21 : 40-44, 2001
6) Ambros IM, Ambros PF, Strehl S, Kovar H, Gadner H, Salzer-Kuntschik M : MIC2 is a specific marker for Ewing's sarcoma and peripheral primitive neuroectodermal tumors. Evidence for a common histogenesis of Ewing's sarcoma and peripheral primitive neuroectodermal tumors from MIC2 expression and specific chromosome aberration. Cancer 67 : 1886-1893, 1991
7) 松谷雅生：New Lecture 3／脳腫瘍，第2版，篠原出版，東京, pp158-163, 1996
8) Grier HE, Krailo MD, Tarbell NJ, Link MP, Fryer CJ, Pritchard DJ, Gebhardt MC, Dickman PS, Perlman EJ, Meyers PA, Donaldson SS, Moore S, Rausen AR, Vietti TJ, Miser JS : Addition of ifosfamide and etoposide to standard chemotherapy for Ewing's sarcoma and primitive neuroectodermal tumor of bone. N Engl J Med 348 : 694-701, 2003
9) de Alava E, Kawai A, Healey JH, Fligman I, Meyers PA, Huvos AG, Gerald WL, Jhanwar SC, Argani P, Antonescu CR, Pardo-Mindan FJ, Ginsberg J, Womer R, Lawlor ER, Wunder J, Andrulis I, Sorensen PH, Barr FG, Ladanyi M : EWS-FLI1 fusion transcript structure is an independent determinant of prognosis in Ewing's sarcoma. J Clin Oncol 16 : 1248-1255, 1998
10) Niwa J, Shimoyama N, Takahashi Y : Primitive neuroectodermal tumor involving the frontal skull base in an infant. Childs Nerv Syst 17 : 570-574, 2001
11) Dedeurwaerdere F, Giannini C, Sciot R, Rubin BP, Perilongo G, Borghi L, Ballotta ML, Cornips E, Demunter A, Maes B, Dei Tos AP : Primary peripheral PNET/Ewing's sarcoma of the dura : a clinicopathologic entity distinct from central PNET. Mod Pathol 15 : 673-678, 2002
12) Antunes NL, Lellouch-Tubiana A, Kalifa C, Delattre O, Pierre-Kahn A, Rosenblum MK : Intracranial Ewing sarcoma/'peripheral' primitive neuroectodermal tumor of dural origin with molecular genetic confirmation. J Neurooncol 51 : 51-56, 2001
13) Papotti M, Abbona G, Pagani A, Monga G, Bussolati G : Primitive Neuroectodermal Tumor of the Meninges : An Histological, Immunohistochemical, Ultrastructural, and Cytogenetic Study. Endocr Pathol 9 : 275-280, 1998
14) Katayama Y, Kimura S, Watanabe T, Yoshino A, Koshinaga M : Peripheral-type primitive neuroectodermal tumor arising in the tentorium. Case report. J Neurosurg 90 : 141-144, 1999
15) Utsunomiya A, Uenohara H, Suzuki S, Shimosaka S, Numagami Y, Nishimura S, Nishino A, Suzuki H, Sakurai Y : [A case of peripheral-type primitive neuroectodermal tumor arising in the dura mater at the frontal base]. No To Shinkei 56 : 237-241, 2004
16) Thomas PR, Perez CA, Neff JR, Nesbit ME, Evans RG : The management of Ewing's sarcoma : role of radiotherapy in local tumor control. Cancer Treat Rep 68 : 703-710, 1984

American Journal of Pathology, Vol. 166, No. 3, March 2005

Tumorigenesis and Neoplastic Progression

Up-Regulation of Angiopoietin-2, Matrix Metalloprotease-2, Membrane Type 1 Metalloprotease, and Laminin 5 γ 2 Correlates with the Invasiveness of Human Glioma

Ping Guo,* Yorihisa Imanishi,* Frank C. Cackowski,* Michael J. Jarzynka,* Huo-Quan Tao,* Ryo Nishikawa,† Takanori Hirose,‡ Bo Hu,§ and Shi-Yuan Cheng*

From the Departments of Pathology and Medicine,§ University of Pittsburgh Cancer Institute, Pittsburgh, Pennsylvania; and the Departments of Neurosurgery† and Pathology,‡ Saitama Medical School, Saitama, Japan*

Diffuse infiltration of malignant human glioma cells into surrounding brain structures occurs through the activation of multigenic programs. We recently showed that angiopoietin-2 (Ang2) induces glioma invasion through the activation of matrix metalloprotease-2 (MMP-2). Here, we report that up-regulation of Ang2, MMP-2, membrane type 1-MMP (MT1-MMP), and laminin 5 γ 2 (LN 5 γ 2) in tumor cells correlates with glioma invasion. Analyses of 57 clinical human glioma biopsies of World Health Organization grade I to IV tumors displaying a distinct invasive edge and 39 glioma specimens that only contain the central region of the tumor showed that Ang2, MMP-2, MT1-MMP, and LN 5 γ 2 were co-overexpressed in invasive areas but not in the central regions of the glioma tissues. Statistical analyses revealed a significant link between the preferential expression of these molecules and invasiveness. Protein analyses of microdissected primary glioma tissue showed up-regulation and activation of MT1-MMP and LN 5 γ 2 at the invasive edge of the tumors, supporting this observation. Concordantly, in human U87MG glioma xenografts engineered to express Ang2, increased expression of MT1-MMP and LN 5 γ 2, along with MMP-2 up-regulation, in actively invading glioma cells was also evident. In cell culture, stimulation of glioma cells by overexpressing Ang2 or exposure to exogenous Ang2 promoted the expression and activation of MMP-2, MT1-MMP, and LN 5 γ 2. These results suggest that up-regulation of Ang2, MMP-2, MT1-MMP, and LN 5 γ 2 is associated with the invasiveness displayed by human gliomas and that induction of these molecules by Ang2 may be essential for glioma invasion. *(Am J Pathol 2005, 166:877–890)*

A hallmark of highly malignant human gliomas is their rapid invasive growth into surrounding brain parenchyma. The infiltration by glioma cells throughout the brain renders these tumors incurable even by the combined approaches of surgery, radiotherapy, chemotherapy, and immunotherapy.[1–3] Studies from both *in vitro* and *in vivo* tumor model systems have suggested a link between increased expression and activation of several matrix metalloproteases (MMPs) such as MMP-2 and membrane type 1 (MT1)-MMP and malignant glioma invasiveness.[4] These MMPs produced by tumor, endothelial, and/or stromal cells degrade extracellular matrix at the invasive fronts of the glioma cells, thus removing the extracellular matrix barrier allowing subsequent tumor cell migration into newly created, more permissive spaces in the adjacent brain structures.[5,6] Additionally, increased expression and activation of laminin (LN) 5 γ 2, a basement membrane protein, has been linked to the invasiveness of malignant human cancers such as breast, lung, pancreatic, colon, esophageal, and cervical cancers.[7] Accumulating evidence demonstrates that interaction between MMP-2 and MT1-MMP leads to the activation of MMP-2[5] and interactions between MMP-2,

Supported by the Brain Cancer Program of James S. McDonnell Foundation, the Sidney Kimmel Foundation for Cancer Research, the National Institutes of Health (grant CA102011), and the American Cancer Society (grant RSG CSM-107144 to S.-Y.C).

Accepted for publication November 15, 2004.

S.-Y.C. is a Kimmel scholar.

Address reprint requests to Shi-Yuan Cheng, Ph.D., Department of Pathology, or Bo Hu, Ph.D., Department of Medicine, University of Pittsburgh Cancer Institute, Research Pavilion at Hillman Cancer Center, Suite 2.26, 5117 Centre Ave., Pittsburgh, PA 15213-1863. E-mail: chengs@upmc.edu or hub@upmc.edu.

MT1-MMP, and LN 5 γ 2 results in the activation of LN 5 γ 2.[8,9] However, the involvement and mechanisms of these proteins in the initiation and maintenance of human glioma cell invasion are not well understood.

Angiopoietin-2 (Ang2) is an angiogenic factor that plays critical roles in angiogenesis and tumor progression. During angiogenesis, Ang2 antagonizes Ang1 activity by competitively inhibiting the binding of Ang1 to their cognate endothelial receptor, Tie2, causing destablization of the vasculature. Ang2 also acts in concert with vascular endothelial growth factor to regulate vessel growth.[10] In human cancers, increased expression of Ang2 in tumor cells is closely correlated to the progression, invasiveness, and metastases of lung, gastric, colon, and breast cancers.[11–15] Stable overexpression of Ang2 by human tumor cells promotes tumor growth, angiogenesis, and metastases in animals.[12,16] We recently have shown that Ang2 induces human glioma cell invasion through the activation of MMP-2 both *in vivo* and *in vitro*. Up-regulated expression of Ang2 and MMP-2 were found in the invasive regions of primary human glioma specimens and in intracranial xenografts of U87MG glioma cells that stably overexpress Ang2.[17] Here, we report that co-expression of Ang2, MT1-MMP, and LN 5 γ 2 were found in the invasive areas, but not in the central regions of primary human glioma specimens. Furthermore, Ang2 induces the expression of MT1-MMP and LN 5 γ 2 in invasive glioma xenografts formed by human U87MG Ang2-expressing glioma cells in the murine brain and in cell culture. These data strongly suggest that Ang2 induces glioma cell invasion through the stimulation of MMP-2, MT-1 MMP, and LN 5 γ 2 in Tie2-deficient glioma cells.

Materials and Methods

Cell Lines and Reagents

Human U87MG glioma cells were obtained from American Type Culture Collection (Rockville, MD) and their culture was previously described.[18] Fetal bovine serum was from HyClone Inc., Salt Lake City, UT. The following reagents were used in this study: anti-Myc-tag antibody (1 μg/ml) from Medical & Biological Laboratories, Ltd., Nagoya, Japan; anti-Ang2 (C-19, 1:50) and anti-LN 5 γ 2 antibodies (C-20, 1:100 or 1 μg/ml) from Santa Cruz Biotechnology, Inc., Santa Cruz, CA; anti-mouse CD31 antibody (MEC 13.3, 1:1000) from BD PharMingen, San Diego, CA; anti-MMP-2 (AB809, 1:100), anti-MT1-MMP antibodies (AB8012, 1:500; AB805, 1:500; and AB815, 1 μg/ml), anti-TIMP-2 antibody (mAb 3310, 1:200) from Chemicon Int., Temecula, CA; anti-MMP-9 antibody (1:1000) from CalBiochem., San Diego, CA; recombinant human Ang2 protein (623-AN-025), anti-Ang2 antibody (AF623, 1:200) from R&D Systems, Minneapolis, MN; and anti-von Willebrand factor (vWF) antibody (1:1000) from DAKO, Carpinteria, CA. The secondary and tertiary antibodies were from Vector Laboratories (Burlingame, CA) or Jackson ImmunoResearch Laboratories (West Grove, PA). A DAB elite kit was from DAKO, Aqua block was from East Coast Biologics, Inc. (North Berwick, ME). Cell culture media and other reagents were from Invitrogen/BRL, Grand Island, New York; Sigma Chemicals, St. Louis, MO; or Fisher Scientific, Hanover Park, IL.

Immunohistochemical (IHC) Analyses of Primary Human Glioma Specimens

Of the 96 human glioma specimens investigated (Table 1 and data not shown), there were 8 pilocytic astrocytomas (PA) [World Health Organization (WHO) grade I], 8 diffuse astrocytomas (DA) (WHO grade II), 3 oligoastrocytomas (OA) (WHO grade II), 7 oligodendrogliomas (OD) (WHO grade II), 10 anaplastic astrocytomas (AA) (WHO grade III), 6 anaplastic oligodendrogliomas (AOD) (WHO grade III), 3 anaplastic oligoastrocytomas (AOA) (WHO grade III), and 51 glioblastoma multiforme (GBM) (WHO grade IV). Among these grade I to IV glioma specimens, 57 samples display an invasive edge and 39 samples contain only the central area of the tumors identified by hematoxylin and eosin (H&E) staining. In addition, four normal human brain specimens were also included as normal controls. All of the tumor samples were surgical specimens obtained during the last 7 years at the Department of Neurosurgery, Saitama Medical School, Saitama, Japan. The normal brain samples were from the cerebral hemisphere or cortex of the brain and obtained through autopsies from patients who did not have any brain lesions. The specimens were fixed in 10% formaldehyde and embedded in paraffin. The WHO glioma grade and the presence of invasive areas in the primary glioma biopsies were verified using H&E-stained tissue sections by Dr. Takanori Hirose, a neuropathologist at the Department of Pathology, Saitama Medical School, Saitama, Japan. The diagnosis of the WHO tumor grade and invasiveness was further confirmed by Dr. Ronald Hamilton, a neuropathologist at the Department of Pathology, University of Pittsburgh, Pittsburgh, PA. The 5-μm sections were deparaffinized in prewarmed xylene (55°C) for 5 minutes followed by dehydration. After washing with Tris-buffered saline, the antigen was retrieved by boiling the sections in a citrate buffer (pH 6.0) twice for 5 minutes. The IHC analyses using diaminobenzidine as a chromogen were performed using anti-Ang2 (C-19), anti-MMP-2 (AB809), anti-MT1-MMP (AB8012), anti-LN 5 γ 2 (C-20), and anti-vWF antibodies as previously described.[17] Quantitative analyses of blood vessel densities were performed on serial-cut human glioma specimens that were stained with the anti-vWF antibody as previously described.[19]

Statistical Analyses

A χ^2 test for trend was performed to examine the association between positive staining for Ang2, MMP-2, MT1-MMP, and LN 5 γ 2 and each area of the glioma specimens (center area, border area, and invasive area) using the StatView Version 5.0 software (SAS Institute Inc., Cary, NC). A two-sided *P* value was calculated on the basis of the χ^2 test. *P* values less than 0.05 were considered significant.

Table 1. Immunohistochemical Staining for Ang2, MMP-2, MT1-MMP, and LN5γ2

Case	Histology (WHO grade)	Ang2			MMP-2			MT1-MMP			LN5γ2		
		Center	Border	Invasion	Center	Border	Invasion	Center	Border	Invasion	Center	Border	Invasion
J140#	Normal	±			−			−			−		
J141#	Normal	±			−			−			−		
J142#	Normal	1+			−			−			−		
J143#	Normal	±			−			−			−		
J39	P.A. (I)	±	2+	1+	2+	2+	2+	−	1+	1+	1+	2+	1+
J40*	P.A. (I)	2+	2+	2+	±	1+	1+	±	1+	±	−	2+	2+
J42	P.A. (I)	−	2+	1+	−	1+	1+	−	1+	1+	−	1+	1+
J43	P.A. (I)	1+	2+	1+	2+	2+	2+	−	1+	1+	1+	2+	2+
J49	P.A. (I)	−	1+	±	±	3+	3+	−	−	−	−	1+	±
J51	P.A. (I)	±	1+	2+	±	1+	2+	−	1+	1+	−	1+	±
J182	P.A. (I)	−	±	±	1+	2+	2+	1+	2+	2+	1+	2+	1+
J13	D.A. (II)	−	3+	1+	−	3+	2+	−	3+	2+	−	3+	1+
J63	D.A. (II)	1+	1+	2+	−	1+	1+	1+	2+	2+	−	1+	1+
J173	D.A. (II)	1+	2+	1+	±	2+	2+	1+	2+	1+	2+	3+	2+
J178	O.A. (II)	1+	2+	1+	±	2+	1+	1+	2+	1+	2+	3+	2+
J19	O.D. (II)	1+	2+	2+	±	2+	1+	±	1+	1+	±	±	±
J48	O.D. (II)	1+	1+	1+	±	1+	2+	±	1+	1+	−	1+	1+
J181	O.D. (II)	±	1+	1+	1+	2+	1+	1+	1+	1+	1+	2+	2+
J10	A.A. (III)	1+	3+	2+	−	1+	1+	±	2+	2+	1+	3+	2+
J11	A.A. (III)	1+	2+	2+	−	1+	1+	−	−	−	2+	2+	2+
J47	A.A. (III)	2+	2+	2+	1+	1+	1+	1+	1+	1+	−	−	±
J60	A.A. (III)	2+	2+	2+	−	±	±	±	±	1+	−	1+	1+
J62	A.A. (III)	1+	2+	2+	1+	1+	2+	±	1+	2+	1+	2+	2+
J165	A.A. (III)	1+	2+	2+	1+	2+	2+	1+	2+	1+	1+	2+	1+
J16	A.O.D. (III)	1+	2+	2+	1+	2+	1+	−	±	−	1+	2+	1+
J17	A.O.D. (III)	2+	3+	3+	1+	2+	1+	±	1+	1+	1+	2+	2+
J95	A.O.D. (III)	1+	2+	2+	±	1+	3+	±	1+	1+	2+	2+	2+
J96	A.O.D. (III)	1+	2+	2+	±	1+	2+	−	1+	±	±	3+	3+
J18	A.O.A. (III)	2+	2+	2+	−	±	±	±	1+	−	2+	2+	3+
J97	A.O.A. (III)	1+	3+	3+	−	1+	1+	±	1+	1+	1+	2+	2+
J1	GBM (IV)	−	2+	2+	−	3+	2+	−	3+	2+	−	3+	2+
J2	GBM (IV)	1+	2+	2+	2+	2+	2+	1+	2+	2+	2+	2+	3+
J3	GBM (IV)	2+	3+	3+	−	1+	2+	±	2+	2+	1+	2+	2+
J5	GBM (IV)	1+	2+	2+	1+	1+	1+	−	±	±	2+	2+	2+
J6	GBM (IV)	2+	3+	2+	2+	2+	2+	±	1+	2+	2+	1+	2+
J7	GBM (IV)	±	2+	2+	1+	2+	2+	1+	1+	2+	1+	2+	2+
J58	GBM (IV)	1+	2+	2+	±	2+	2+	±	2+	1+	−	2+	2+
J64	GBM (IV)	±	2+	±	−	1+	1+	−	1+	−	±	2+	1+
J66	GBM (IV)	1+	2+	2+	2+	2+	2+	−	1+	1+	1+	1+	2+
J68	GBM (IV)	1+	2+	2+	2+	2+	2+	±	1+	1+	1+	2+	2+
J71	GBM (IV)	2+	3+	3+	±	2+	2+	−	1+	1+	±	±	1+
J72	GBM (IV)	±	2+	2+	1+	2+	1+	−	1+	1+	1+	1+	1+
J78	GBM (IV)	2+	2+	3+	1+	2+	1+	−	1+	1+	−	1+	1+
J79	GBM (IV)	2+	3+	3+	−	−	−	−	1+	1+	1+	2+	2+
J80	GBM (IV)	1+	2+	2+	±	2+	1+	−	±	±	1+	2+	2+
J81	GBM (IV)	1+	3+	3+	1+	2+	2+	−	1+	1+	1+	2+	2+
J82	GBM (IV)	2+	3+	3+	±	2+	1+	−	1+	1+	−	1+	1+
J83	GBM (IV)	±	2+	2+	±	1+	2+	−	1+	1+	2+	2+	2+
J85	GBM (IV)	2+	3+	2+	−	1+	1+	1+	1+	2+	1+	2+	1+
J86	GBM (IV)	2+	3+	3+	1+	2+	2+	±	1+	1+	1+	2+	1+
J87	GBM (IV)	1+	1+	2+	±	2+	1+	1+	2+	2+	2+	2+	±
J89	GBM (IV)	1+	2+	1+	1+	2+	2+	1+	2+	2+	±	1+	1+
J94	GBM (IV)	1+	2+	2+	1+	2+	2+	−	1+	1+	±	2+	2+
J98	GBM (IV)	1+	2+	2+	1+	1+	2+	1+	1+	2+	1+	1+	1+
J151	GBM (IV)	2+	2+	2+	−	2+	2+	−	1+	1+	1+	2+	2+
J152	GBM (IV)	1+	2+	2+	1+	2+	1+	1+	2+	2+	1+	2+	2+
J153	GBM (IV)	1+	3+	2+	±	2+	1+	−	1+	1+	2+	3+	3+
J154	GBM (IV)	1+	2+	2+	1+	3+	2+	1+	2+	2+	1+	2+	2+
J155	GBM (IV)	1+	2+	2+	1+	2+	1+	±	2+	2+	±	2+	1+
J156	GBM (IV)	2+	3+	3+	2+	2+	3+	1+	2+	2+	1+	2+	2+
J164	GBM (IV)	1+	2+	2+	1+	3+	2+	±	1+	1+	±	2+	1+

*Contains neurofibroma 1.
#Scores of normal brain were indicated in the columns of "Center" for convenience.
P.A., pilocytic astrocytoma; D.A., diffuse astrocytoma; O.A., oligoastrocytoma; O.D., oligodendroglioma; A.A., anaplastic astrocytoma; A.O.D., anaplastic oligodendroglioma; A.O.A., anaplastic oligoastocytoma; GBM, glioblastoma multiforme.

Microdissection of Paraffin-Embedded Tissue Sections of Human Glioma Specimens

Microdissection of paraffin-embedded primary human glioma tissues was performed as previously described.[20] Briefly, paraffin-embedded glioma specimens were sectioned separately at 5 μm and 50 μm thickness and mounted onto plain glass slides. To identify the center, border, and invasion regions within the glioma specimen, 5-μm-thick sections were stained by H&E. Three 50-μm-thick sister sections of each sample were then deparaffinized in xylenes, rehydrated in graded ethanol, immersed in distilled water, and air-dried. To exclusively collect center-tumor or border-tumor tissues, the targeted areas were cut microscopically under an Olympus SZ-STS stereomicroscope (Melville, NY) with a fine needle referring to the microscopic observation of the morphology of serial H&E-stained sections.

Extraction and Western Blot Analyses of Proteins from Microdissected Human Primary Glioma Tissues

Protein extraction from microdissected formalin-fixed, paraffin-embedded tissues was performed following protocols that were previously described.[21] Briefly, the collected tumor tissues were suspended in lysis buffer containing 25 mmol/L sodium phosphate buffer (pH 7.6), 150 mmol/L sodium chloride, 1% Triton X-100, 2% sodium dodecyl sulfate, 12 mmol/L sodium deoxycholate, 0.2% sodium azide, 0.95 mmol/L fluoride, 2 mmol/L phenylmethyl sulfonyl fluoride, 50 mg/ml aprotinin, and 50 mmol/L leupeptin and incubated at 100°C for 20 minutes followed by incubation at 60°C for 2 hours. After incubation, the tissue lysates were centrifuged at 15,000 × *g* for 20 minutes at 4°C, and the supernatants containing extracted proteins were collected. The protein extracts were then subjected to Western blot analyses using a sensitive protocol.[22] Briefly, 10 μg of total proteins were separated by NuPAGE 4 to 12% Bis-Tris polyacrylamide gels (Invitrogen) and transferred to Immobilon-P transfer membranes (pore size 0.45 μm; Millipore, Bedford, MA) according to the manufacturer's standard procedure. The membrane was blocked and separately probed with anti-MT1-MMP (AB8012, Chemicon), anti-LN 5 γ 2 (C-20, Santa Cruz Biotechnology), and anti-β-actin (Sigma) antibodies. Antibody detection was accomplished with SuperSignal West Femto maximum sensitivity substrate (Pierce).

Generation of U87MG Cell Lines That Stably Express Ang2 or LacZ

Transfected U87MG cell clones that stably express Ang2 were generated by transfecting U87MG cells with a cDNA for Ang2 in the pSecTagB/Myc-His(+) expression vector (Invitrogen, San Diego, CA). The clones that expressed exogenous biologically active Ang2 or LacZ were expanded and characterized as previously described.[17,18]

Tumorigenicity, Glioma Invasion, Mouse Brain Tissue Processing, and IHC

U87MG LacZ- or U87MG Ang2-expressing cell clones (5×10^5) were stereotactically implanted into individual nude mouse brains with five mice per group. When mice developed neurological symptoms because of disturbance of their central nervous system, mice were sacrificed and their brains were removed, processed, and analyzed by IHC as previously described.[17,18]

Quantification Analyses of IHC Data

To quantify microvascular density or the degree of staining by antibodies (for mouse xenograft tissues), five to seven serial-cut sections were stained with the anti-CD31, anti-vWF, anti-Ang2, anti-MMP-2, anti-MT1-MMP, or anti-LN 5 γ 2 antibodies. The stained images (10 or more random areas per section) were captured using an Olympus BX51 microscope equipped with a digital camera, imported into the Image Pro Plus program (Version 4.1; Media Cybernetics, Silver Spring, MD) and analyzed. The mean values of microvessel density or relative intensity of antibody staining from serial brain sections (five or more individual mice per group) in each group were used. Microvessel density was expressed as the ratio of positively stained areas to the total area of the image (object areas/mm^2).[19] The degree of antibody staining in U87MG/Ang2 gliomas was shown as fold of increase to that in U87MG/LacZ tumors.[17]

To quantify the intensities of IHC staining on primary human glioma specimens using anti-Ang2, anti-MMP-2, anti-MT1-MMP, and anti-LN 5 γ 2 antibodies, two experienced researchers (P.G. and Y.I.) independently examined all of the aforementioned sections stained with the four antibodies under ×200 and ×400 magnification. In each stained section, 5 to 10 identified areas (center area, border area, and invasive area) in each type were examined. The intensities of IHC staining with each antibody were defined as no stain (−), weakest (±), low (1+), medium (2+), and strong (3+) stains. The immunoactivities of each antibody on the paraffin-embedded sections were different. The anti-Ang2 and anti-MMP-2 antibodies produced excellent staining without nonspecific background staining. The anti-MT1-MMP had the weakest activity whereas the anti-LN 5 γ 2 antibody had nonspecific staining in some tissue areas. These variations were considered during the scoring. Greater than 95% of the scoring by the two examiners determined in a double-blinded manner was comparable. Discrepancies between the scores were resolved by re-examining the stained sections side-by-side followed by consultation between the examiners.

Western Blot and Zymography Analyses

Western blot and zymography analyses were performed as previously reported.[17] Briefly, six-well plates were coated with or without 10 μg/ml of recombinant Ang2 or bovine serum albumin in phosphate-buffered saline

(PBS) at 4°C overnight, washed three times with PBS, and then dried. U87MG cells or U87MG Ang2-expressing cells were seeded onto the plates and incubated in Dulbecco's modified Eagle's medium with 10% heat-inactivated cosmic calf serum for 4 hours at 37°C. The medium was then replaced by serum-free Dulbecco's modified Eagle's medium, and the cells were maintained in the medium for 24 hours at 37°C. Whole cell lysates containing 30 μg of total protein from the various cells were separated by sodium dodecyl sulfate-polyacrylamide gel electrophoresis under reducing conditions and transferred onto a nitrocellulose membrane. The membrane was blocked and probed with various antibodies. The reacted proteins were visualized by enhanced chemiluminescence reaction. Quantification of the expression of MT1-MMP, TIMP-2, and LN 5 γ 2 was performed by importing and analyzing the scanned images using the Image Pro Plus program.

The zymography analysis for proteolytic activities of MMP-2 toward gelatin was performed as previously described.[17] Briefly, serum-free conditioned medium from a 48-hour culture of various U87MG cells plated onto six-well plates coated with Ang2, bovine serum albumin, or noncoating was collected. Conditioned medium containing 20 μg of total proteins was separated at 4°C in a 7.5% sodium dodecyl sulfate polyacrylamide gel containing 0.2% gelatin. The sodium dodecyl sulfate in the gel was removed by washing the gel three times with a Tris-HCl buffer containing 2% Triton X-100. The gel was rinsed and developed in a gel-developing buffer containing 1% Triton X-100 and 5 mmol/L of $CaCl_2$ at 37°C for 16 hours. The gel was then stained by a Coomassie Blue solution, destained, and photographed. The proteolytic activities of MMP-2 toward gelatin appear as unstained areas.

Results

Preferential Expression of Ang2, MMP-2, MT1-MMP, and LN 5 γ 2 in Invading Glioma Cells and Neovessels of Human Primary Glioma Specimens

We recently reported that Ang2 and MMP-2 are co-overexpressed in the invasive areas including tumor borders, but not in the central regions of primary human glioma biopsies.[17] To further demonstrate whether there is a significant association between up-regulated expression of Ang2, MMP-2, MT1-MMP, and LN 5 γ 2 and tumor invasiveness displayed by various human gliomas in all four WHO grade stages, we conducted a comprehensive survey by IHC analyses. The IHC analyses were performed on a total of 96 human glioma specimens and 4 normal human brain biopsies in our collection. We tested several well-characterized antibodies against each of these molecules that have been reported in similar clinical investigations on human tumor specimens and chose goat anti-Ang2 (C-19),[11,12,15] rabbit anti-MMP-2 (AB809),[9,23] rabbit anti-MT1-MMP (AB8012),[9,23] and goat anti-LN 5 γ 2 (C-20) antibodies as described in the Materials and Methods section. For the negative controls, we applied isotype-matched IgG at the same concentration onto the sister sections of each specimen during the IHC staining, which all showed negative stains (see the insets in Figure 2). The specificity of each of these antibodies on detecting the corresponding protein products were verified by Western blot analyses using these antibodies on U87MG cells that express endogenous MMP-2, MT1-MMP, and LN 5 γ 2 proteins (Figure 4, and data not shown) and U87MG Ang2-expressing cells (for Ang2).[17] Table 1 summarizes our findings of the relative immunoactivities of Ang2, MMP-2, MT1-MMP, and LN 5 γ 2 in 57 paraffin-embedded biopsies of human gliomas that display invasiveness or normal human brain specimens. The relative intensities of the immunostaining by each antibody were quantified as described in the Materials and Methods section.

Normal Human Brain Tissues

We performed IHC analyses on four normal brain samples that were from autopsied patients who did not have brain lesions (specimens J140 to J143, Table 1). All four specimens were mostly from the cerebral hemisphere or cortex of the brain where gliomas occur most frequently.[3] These specimens were homogenous normal brain tissue with similar morphology judged by H&E staining (Figure 1a). As shown in Figure 1 (specimen J141) and Table 1, no or very weak immunoactivities of the antibodies to Ang2 (Figure 1b), MMP-2 (Figure 1d), MT1-MMP (Figure 1e), or LN 5 γ 2 (Figure 1g) were detected. These data indicate that under normal physiological conditions, the expression of these molecules is below or near the detectable levels by IHC analyses.

Pilocytic Astrocytomas (WHO Grade I)

Eight PA biopsies were included in this study (specimens J39, J40, J42, J43, J49, J51, J182, and J183). By H&E staining, we found distinct invasive areas in seven of eight PA biopsies (87.5%; Table 1, data not shown). In addition, intratumoral hemorrhage is common in most of these grade I tumors (Figure 2A, b, data not shown). Figure 2A shows the IHC staining of specimen J42 using H&E and various antibodies. In the center regions of this PA, low expression of Ang2 (Figure 2A, d), MMP-2 (Figure 2A, g), MT1-MMP (Figure 2A, j), and LN 5 γ 2 (Figure 2A, m) was detected (Table 1). In the tumor border (Figure 2A, b), increased expression levels of Ang2 (Figure 2A, e), MMP-2 (Figure 2A, h), and LN 5 γ 2 (Figure 2A, n) are found while a low level of MT1-MMP expression was seen (Figure 2A, k). Interestingly, high levels of Ang2 and MMP-2, but not MT1-MMP and LN 5 γ 2, were seen in neovessels (arrowheads in Figure 2A, e and h), suggesting the role of Ang2 and MMP-2 in vascular growth. In invasive areas (0.25 mm away from the border, Figure 2A, c) where glioma cells are actively invading into the brain structure, only tumor cells express Ang2 (Figure 2A, f, arrows), MMP-2 (Figure 2A, i, arrows), MT1-MMP (Figure 2A, l, arrows), and LN 5 γ 2 (Figure 2A, o, arrows).

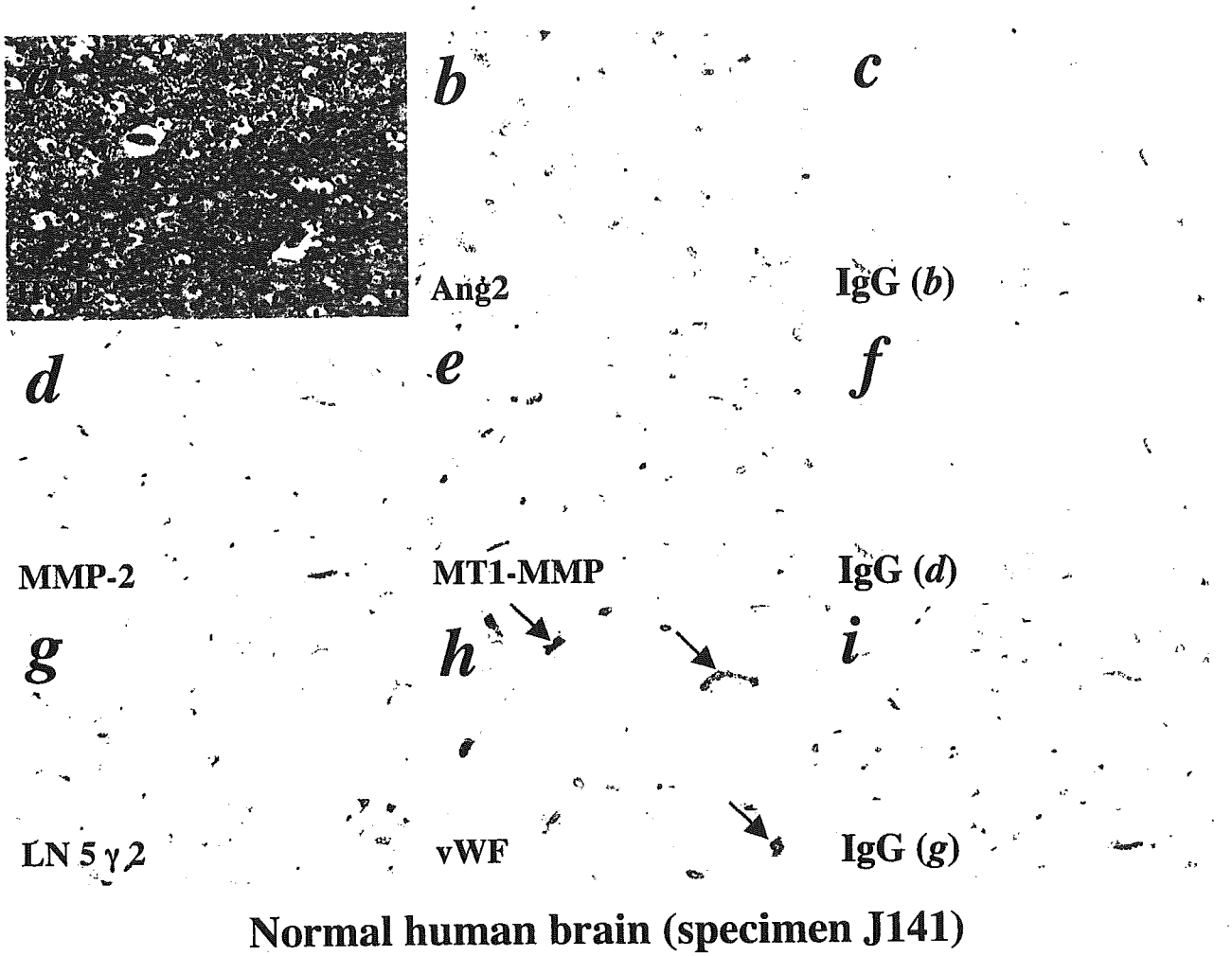

Figure 1. Expression of Ang2, MMP-2, MT1-MMP, and LN 5 γ 2 in normal human brain tissue. IHC on serial sections of a normal human brain biopsy (specimen J141) using H&E (**a**), goat polyclonal anti-Ang2 (**b**), rabbit polyclonal anti-MMP-2 (**d**), rabbit polyclonal anti-MT1-MMP (**e**), goat anti-LN 5 γ 2 (**g**), and rabbit polyclonal anti-vWF (**h**) antibodies. The isotype-matched IgG controls (**c**, **f**, and **i**) are the identical areas shown in **b**, **d**, and **g**. **Arrows** in **h** indicate blood vessels. A total of four individual normal human brain tissues were analyzed. The experiments were repeated two additional times with similar results. Original magnifications, ×400.

Thus, co-expression of Ang2, MMP-2, MT1-MMP, and LN 5 γ 2 are detected in the invading glioma cells and growing neovessels in tumor borders, but not in the central regions of PA tumors. These results suggest that at the early stage of glioma progression, up-regulation of these molecules correlates with the initial invasion displayed by PA.

Diffuse Astrocytomas (DA, Grade II), Oligoastrogliomas (OA, Grade II), and Oligodendrogliomas (OD, Grade II)

There were 8 DA, 3 OA, and 7 OD biopsies that are WHO grade II tumors in our collection. In the DA specimens, diffuse morphology of tumor cells is evident. In some tumors, diffusive tumor cells formed a cellular gradient toward the normal brain structure without identifiable borders (data not shown). Among the 18 grade II tumors, 7 tumor specimens (38.8%) contain identifiable tumor borders and clear invasive regions (at least 0.25 mm away from the tumor border, Table 1). Figure 2B shows the IHC staining of specimen J13 (a DA) using H&E and various antibodies. Consistent with the expression profiles in the WHO grade I gliomas (Figure 2A), strong expression of Ang2 (Figure 2B, e), MMP-2 (Figure 2B, h), MT1-MMP (Figure 2B, k), and LN 5 γ 2 (Figure 2B, n) were evident in tumor cells (arrows) and in neovessels (arrowheads) along the tumor border, but not in the center region of the tumors (Figure 2B; d, g, j, and m). Increased expression of Ang2 (Figure 2B, f), MMP-2 (Figure 2B, i), and LN 5 γ 2 (Figure 2B, o), and strong expression of MT1-MMP (Figure 2B, l) were detected in cells (arrows in Figure 2B; f, i, l, and o) and in vessels (arrowheads) in the invasive areas that are 0.25 mm away from the tumor border.

Anaplastic Astrocytomas (AA, Grade III), Anaplastic Oligodendrogliomas (AOD, Grade III), and Anaplastic Oligoastrocytomas (AOA, Grade III)

There were 10 AA, 6 AOD, and 3 AOA gliomas in our collection. All of the grade III gliomas displayed in-

creased cellularity and malignancy, especially in the central region (data not shown). Among the 19 grade III glioma biopsies, 12 tumors contain tumor borders and invasive areas (63.2%, Table 1). In contrast to the grade I and II glioma specimens, the tumor borders were distinct and with sharp edges (data not shown). Similar to that in the grade II gliomas (Figure 2B), up-regulated Ang2, MMP-2, MT1-MMP, and LN 5 γ 2 were found in the tumor borders, but not in the central regions of these tumors (data not shown). In addition, increased expression of all four molecules were detected in cells in the invasive region 0.25 mm away from the tumor borders in the grade III gliomas (data not shown).

GBM (WHO Grade IV)

There were 51 GBM specimens in our collection. These grade IV glioma biopsies display the highest cellularity and contain evident necrotic areas and intratumoral hemorrhage (data not shown). Among the 51 GBM, 31 specimens contain tumor borders and invasive areas (60.8%, Table 1). The tumor borders are also sharp and easily distinguishable (Figure 2C, a). Figure 2C shows the IHC staining of specimen J1 (a GBM) using H&E and various antibodies. We found that protein expression profiles of Ang2 (Figure 2C, e), MMP-2 (Figure 2C, h), MT1-MMP (Figure 2C, k), and LN 5 γ 2 (Figure 2C, n) were located in the tumor borders similar to IHC staining of the grade II and III gliomas (Figure 2B and data not shown). In addition, increased levels of expression of Ang2 (Figure 2C, f), MMP-2 (Figure 2C, i), MT1-MMP (Figure 2C, l), and LN 5 γ 2 (Figure 2C, o) were also found in the invasive areas of the GBM tumors. The IHC results of WHO grade III and IV gliomas demonstrate that increased expression of Ang2, MMP-2, MT1-MMP, and LN 5 γ 2 are further elevated in the tumor borders and invasive regions of high-grade human glioma specimens.

Glioma Angiogenesis

As shown in Figures 1 and 2, we stained all of the normal brain and glioma tissue specimens using an anti-vWF antibody that stains tumor endothelium. We evaluated glioma angiogenesis by quantifying the microvessel density in all of the stained tissue sections. In normal human brain tissues, vessels were apparent (Figure 1, h). In WHO grade I (Figure 2A, p and q) and II (Figure 2B, p and q) tumors, when compared with the MCD in normal brain tissues, a 1.8-fold increase of MCD was found. In WHO grade III gliomas, a 3.2-fold increase of MCD was seen. In WHO grade IV gliomas (Figure 2C, p and q), a further increase of MCD (7.1-fold) was found (data not shown). These data corroborate with previous studies showing that glioma angiogenesis is not evident in low-grade (I and II) gliomas, but significantly increased in high-grade (III and IV) tumors.[24]

Up-Regulated Ang2, MMP-2, MT1-MMP, and LN 5 γ 2 Are Preferentially Associated with Tumor Invasiveness among the Clinical Glioma Specimens

As shown in Table 1, we have found that 57 glioma specimens contain identifiable tumor borders and nearby invasive regions. There are 39 additional glioma specimens that only contain the central region of the tumors. We hypothesize that there is a significant association between up-regulated expressions of Ang2, MMP-2, MT1-MMP, and LN 5 γ 2 and tumor invasiveness displayed by all four WHO grades of human gliomas. To test our hypothesis, we examined the IHC analyses data on the cases that contain all three areas within the same sample: tumor center, border, and invasive areas, and determined the number of the cases analyzed that meet these criteria. As shown in Table 1, in seven grade I gliomas, there are five to six cases of seven samples (71 to 85.7%) that have expression scores in the areas both in the border and invasive areas higher than that of the center area. Similarly, the scores of protein expression level in the majority of cases in grade II to IV specimens meet the same criteria: grade II, 5 to 6 cases of 7 (71 to 85.7%); grade III, 7 to 9 cases of 12 (58 to 75%), and grade IV, 23 to 28 cases of 31 (74.1 to 90%). Together, in a total of 50 glioma grade II to IV specimens that contain all three areas (center, border, and invasion), 35 to 43 cases (70 to 86%) are available for testing our hypothesis (Table 2).

Next, we determined whether there is a distinct link between the up-regulation of the four molecules that are shown to be vital in the invasiveness of human cancers. A χ^2 test for trend was performed to examine the association between positive staining for Ang2, MMP-2, MT1-MMP, LN 5 γ 2, and each area of grade II to IV glioma specimens (center area, border area, and invasion area). A two-sided P value was calculated on the basis of the χ^2 test. As shown in Table 2, significant links are found between the positive immunoactivities of Ang2 ($P < 0.0001$ for both comparisons), MMP-2 ($P < 0.0001$ for border versus center and $P = 0.0001$ for invasion versus center, respectively), MT1-MMP ($P < 0.0001$ for both comparisons), and LN 5 γ 2 ($P < 0.0001$ for border versus center and $P = 0.0002$ for invasion versus center, respectively), and the invasiveness displayed by these gliomas. In contrast, there are no differences in the expression profiles of these four proteins between the tumor borders and invasive regions (between $P = 0.5120$ to $P = 0.7880$). Because the pathogenesis of PAs is different from that of grade II to IV gliomas,[3] we separately performed the χ^2 test for trend on the IHC data for PA gliomas. No significant association of the expression levels of these four molecules and tumor invasiveness could be found, possibly because of the small sample size analyzed (data not shown). In addition, because the majority of the glioma specimens analyzed in Table 2 are grade IV GBM (31 of 50, 62%), we separately performed the χ^2 test for trend analyses on the IHC data of these 31 grade IV GBM samples. A statistically significant link

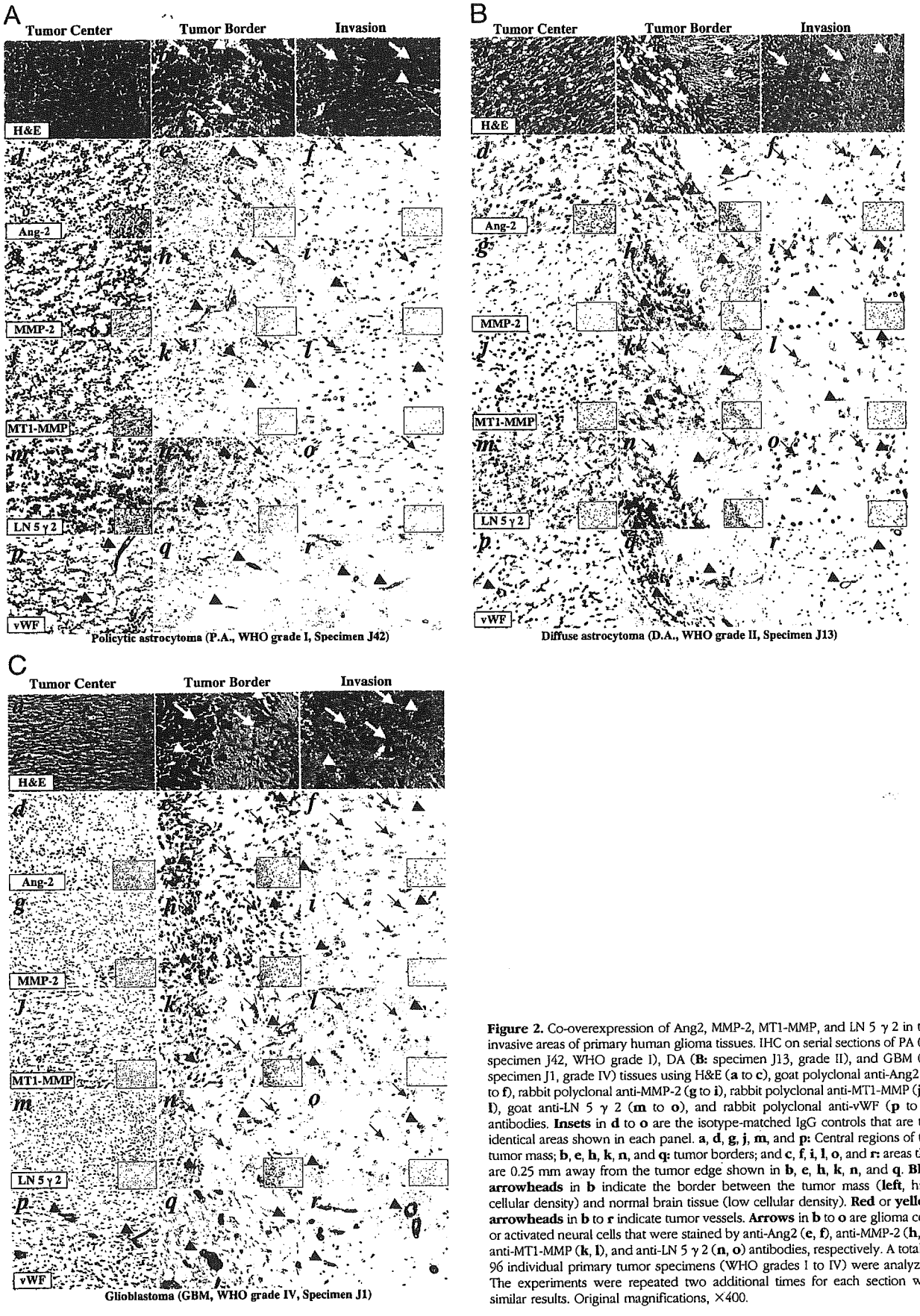

Figure 2. Co-overexpression of Ang2, MMP-2, MT1-MMP, and LN 5 γ 2 in the invasive areas of primary human glioma tissues. IHC on serial sections of PA (**A:** specimen J42, WHO grade I), DA (**B:** specimen J13, grade II), and GBM (**C:** specimen J1, grade IV) tissues using H&E (**a** to **c**), goat polyclonal anti-Ang2 (**d** to **f**), rabbit polyclonal anti-MMP-2 (**g** to **i**), rabbit polyclonal anti-MT1-MMP (**j** to **l**), goat anti-LN 5 γ 2 (**m** to **o**), and rabbit polyclonal anti-vWF (**p** to **r**) antibodies. **Insets** in **d** to **o** are the isotype-matched IgG controls that are the identical areas shown in each panel. **a**, **d**, **g**, **j**, **m**, and **p:** Central regions of the tumor mass; **b**, **e**, **h**, **k**, **n**, and **q:** tumor borders; and **c**, **f**, **i**, **l**, **o**, and **r:** areas that are 0.25 mm away from the tumor edge shown in **b**, **e**, **h**, **k**, **n**, and **q**. **Blue arrowheads** in **b** indicate the border between the tumor mass (**left**, high cellular density) and normal brain tissue (low cellular density). **Red** or **yellow arrowheads** in **b** to **r** indicate tumor vessels. **Arrows** in **b** to **o** are glioma cells or activated neural cells that were stained by anti-Ang2 (**e**, **f**), anti-MMP-2 (**h**, **i**), anti-MT1-MMP (**k**, **l**), and anti-LN 5 γ 2 (**n**, **o**) antibodies, respectively. A total of 96 individual primary tumor specimens (WHO grades I to IV) were analyzed. The experiments were repeated two additional times for each section with similar results. Original magnifications, ×400.

Table 2. Scores and Correlation between Positivity for Staining and Each Area of Tumor (Grade II–IV, $n = 50$)

	Ang2			MMP-2			MT1-MMP			LN5γ2		
	Center	Border	Invasion	Center	Border	Invasion	Center	Border	Invasion	Center	Border	Invasion
3+	0	14	11	0	2	3	0	0	0	0	5	4
2+	14	32	33	5	29	22	0	16	16	11	31	27
1+	31	4	5	19	16	22	17	29	27	22	11	16
±	5	0	1	15	2	2	16	4	3	9	2	3
−	0	0	0	11	1	1	17	1	4	8	1	0
P value of correlation between positivity and area of tumor*												
Border vs center		<0.0001			<0.0001			<0.0001			<0.0001	
Invasion vs center		<0.0001			0.0001			<0.0001			0.0002	
Border vs invasion		N.S.			N.S.			N.S.			N.S.	

*Analyzed by χ^2 test for trend based on the distribution of the scores of each area.
N.S., not significant.

between the expression profiles of Ang2, MMP-2, MT1-MMP, and LN 5 γ 2 and invasiveness of these GBM was also found ($P < 0.0001$ to $P = 0.0159$ for border versus center or invasion versus center). Similarly, there is no difference in the immunoactivities of these four molecules between the border and invasive areas ($P = 0.3939$ to $P = 0.9996$, data not shown).

Lastly, we assessed the protein expression levels in the 39 cases of grade II to IV gliomas that only have the center area, but no tumor border and invasive area. Among these 39 samples, 25 to 33 cases (64.1 to 84.6%) have low levels of protein expression of the four molecules that were examined (scores ≤1+, data not shown). Because we do not have portions of these glioma biopsies containing tumor border and invasion areas, we cannot evaluate the correlation of the expression levels of Ang2, MMP-2, MT1-MMP, and LN 5 γ 2 with the invasive edge in these 39 human glioma specimens.

MT1-MMP and LN 5 γ 2 Are Overexpressed and Activated in the Invasive Region of Primary Human Glioma Specimens

To support our observations from the IHC analyses, we identified five primary human glioma specimens from our collection that have shown increased co-expression of Ang2, MMP-2, MT1-MMP, and LN 5 γ 2 in the invasive regions (Table 1) with sufficient tumor material: J181, WHO grade II OD; J165, a grade III AA; J152, a grade IV GBM; J152, a grade IV GBM; and J155, a grade IV GBM. We microdissected the tissues of the central region and the invasive edge of these primary glioma specimens (Figure 3A).[20] Then, we performed Western blot analyses on the total proteins extracted from the microdissected glioma tissue samples using anti-MT1-MMP and anti-LN 5 γ 2 antibodies according to the protocols that were previously reported.[21,22] As shown in Figure 3B, a twofold to threefold increase in protein expression of intact MT1-MMP (70 kd) was found in the samples from the tumor invasive edge of all of the five primary glioma specimens when compared with the central regions in the same sample. Furthermore, significant proteolytic activation of LN 5 γ 2 (155 kd) was evident by the appearance of γ2′ (105 kd) and γ2x (90 kd) fragments[8] in the samples of the tumor invasive edge of all five specimens. Autocleaved MT1-MMP protein fragments (45 kd) were also detected, albeit to a lesser degree, indicating that activation of LN 5 γ 2 and MT1-MMP occurred in these regions of the gliomas. These findings corroborate with the IHC data shown in Figure 2 and Table 1 that MT1-MMP and LN 5 γ 2 are co-up-regulated and co-activated with Ang2 and MMP-2 in the invasive edge of primary human glioma grade II to IV specimens. Taken together, our results (Tables 1 and 2 and Figures 1 to 3) demonstrate that up-regulation of Ang2, MMP-2, MT1-MMP, and LN 5 γ 2 are preferentially associated with the invasive edge of WHO grade I to IV gliomas.

MT1-MMP and LN 5 γ 2 Are Overexpressed at the Invasive Fronts and Disseminated U87MG Ang2-Expressing Gliomas in the Brain

We recently reported that overexpression of Ang2 by human U87MG glioma cells caused aggressive glioma invasion compared to isogenic control tumors. We found that Ang2 and MMP-2 were co-overexpressed in the actively invading regions of U87MG Ang2-expressing tumors.[17] To determine whether the expressions of MT1-MMP and LN 5 γ 2 were also up-regulated in the invasive regions of the Ang2-expressing U87MG gliomas, we performed IHC on various U87MG gliomas. As shown in Figure 4, the expression of MT1-MMP (Figure 4, f) and LN 5 γ 2 (Figure 4, h) was co-overexpressed with Ang2 (Figure 4, d) in the Ang2-expressing gliomas, whereas neither of these two proteins was detected in the isogenic control tumors (LacZ-expressing tumors; Figure 4, e and g). Because both MT1-MMP (Figure 4, f) and LN 5 γ 2 (Figure 4, h) are extracellular matrix proteins, the protein stains detected in the invasive Ang2 tumors were relatively diffusive. The highest expressions of MT1-MMP and LN 5 γ 2 (a fourfold to fivefold increase compared to that in LacZ tumors) were found at the invasive fronts as well as in the disseminated tumor clusters of the U87MG/Ang2 gliomas (arrows in Figure 4, f and h). Importantly, high expression of MT1-MMP (Figure 4, f) and LN 5 γ 2

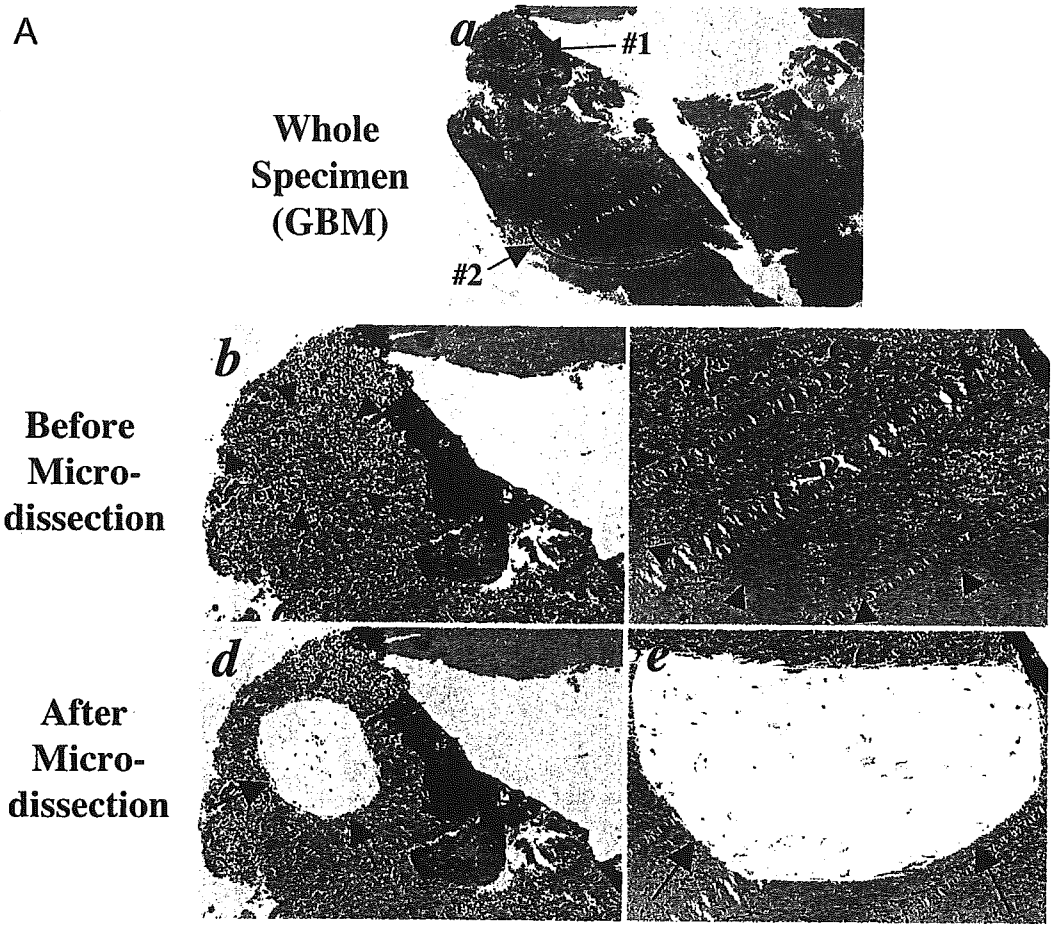
A
Whole Specimen (GBM)
a
#1
#2
Before Micro-dissection
b
c
After Micro-dissection
d
e

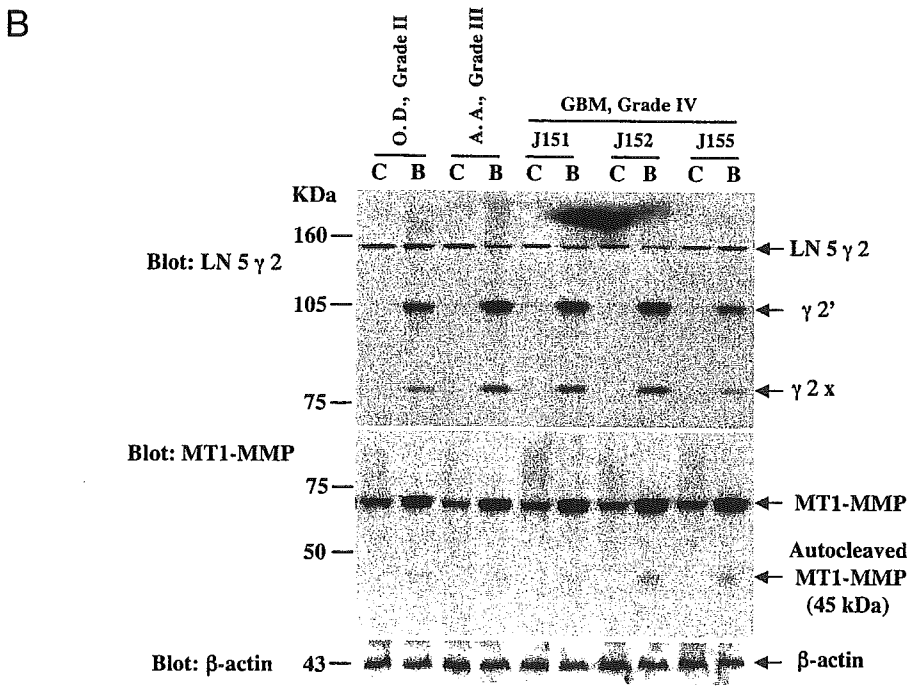
B
O. D., Grade II
A. A., Grade III
GBM, Grade IV
J151
J152
J155
C B C B C B C B C B
KDa
160
105
75
Blot: LN 5 γ 2
LN 5 γ 2
γ 2'
γ 2 x
Blot: MT1-MMP
75
50
MT1-MMP
Autocleaved MT1-MMP (45 kDa)
Blot: β-actin
43
β-actin

(Figure 4, h) are not only co-localized in the invading malignant cells or disseminated tumor clusters, but also co-expressed in the same cell population where Ang2 (Figure 4, d) and MMP-2 are overexpressed.[17] Co-overexpression of these four molecules in the regions where Ang2-induced gliomas invasion occurs suggests that Ang2 induces human glioma invasion through the activation of the downstream effectors MMP-2, MT1-MMP, and LN 5 γ 2.

Ang2 Induces the Stimulation of MT1-MMP and LN 5 γ 2 in Vitro

Increased expression and activation of both MT1-MMP and LN 5 γ 2 are strongly associated with tumor invasion in various types of human cancers.[7,25] To determine whether Ang2 can directly stimulate the expression and activation of MT1-MMP and LN 5 γ 2 in glioma cells, we assessed the expression and proteolysis of these two molecules in various conditions. As shown in Figure 5, overexpression of Ang2 by U87MG cells or exposure to recombinant Ang2 by U87MG, U251MG, and T98G cells (data not shown) results in a 2.2- to 3.4-fold increase in expression and activation of LN 5 γ 2 (Figure 5, top) and MT1-MMP (Figure 5, the second panel) in comparison to untreated or bovine serum albumin-treated U87MG cells. Importantly, the stimulation of both MT1-MMP and LN 5 γ 2 under these conditions correlates with increased expression and activation of MMP-2 in the glioma cells (Figure 5, bottom). Because MT1-MMP is responsible for the activation of MMP-2 by interacting with tissue inhibitor-2 of MMP (TIMP-2),[5] we also determined the expression of TIMP-2 in the glioma cells under these conditions and in the invasive U87MG/Ang2 and noninvasive U87MG/LacZ gliomas. We found that there was no alteration in the expression levels of TIMP-2 in Ang2-stimulated or nonstimulated glioma cells (Figure 5, the third panel), nor in the invasive or noninvasive U87MG gliomas established in the mouse brain (data no shown). Therefore, similar to that of MMP-2,[17] the stimulation of MT1-MMP and LN 5 γ 2 is involved in human glioma invasion induced by Ang2 *in vitro* and *in vivo*.

Discussion

The involvement of Ang2, MMP-2, MT1-MMP, and LN 5 γ 2 in the invasiveness of various human cancers including gliomas has been intensively investigated using clinical tumor specimens, xenografts of human tumor cells, and cell culture models.[5,7,12,15,25,26] However, most of the studies focused on the roles of only one or two of these molecules in human tumor invasion and metastases. In this report, we use three distinct model systems to determine whether there is a significant link between the expression profiles and four important molecules, Ang2, MMP-2, MT1-MMP, and LN 5 γ 2 and human glioma invasion. First, we performed a comprehensive survey of the expression profiles of Ang2, MMP-2, MT1-MMP, and LN 5 γ 2 by analyzing a total of 96 primary human glioma specimens that included 57 samples containing a distinct invasive edge and 39 glioma biopsies containing only central regions of the tumor, and 4 normal brain biopsies. Statistical analysis of our results establishes that there is a significant association between the up-regulated expression of these molecules and the invasiveness of the various gliomas in all four WHO grades. Additionally, low levels of protein expression of these four molecules were detected in the central areas of the majority of these clinical glioma samples. Second, Western blot analyses of microdissected primary glioma specimens showed that MT1-MMP and LN 5 γ 2 proteins were not only co-up-regulated but also co-activated in the cells consisting of the invasive edge of the tumor when compared with the center regions of the same sample, thus supporting our findings of IHC analyses. Third, we further analyzed our recently established glioma invasion animal model[17] and showed that the aggressively invasive U87MG Ang2-expressing gliomas were accompanied by up-regulated MMP-2, MT1-MMP, and LN 5 γ 2 in tumor cells that are actively invading the brain. Finally, stimulation of human glioma cells by overexpressing Ang2 or exposure to exogenous Ang2 induced the expression and activation of MT1-MMP, MMP-2, and LN 5 γ 2 in glioma cells *in vitro*. Together, our data provide evidence suggesting that up-regulation of Ang2, MMP-2, MT1-MMP, and LN 5 γ 2 in actively invading tumor cells correlates with human glioma invasion and stimulation of MMP-2, MT1-MMP, and LN 5 γ 2 are involved in Ang2-induced glioma invasion.

MMP-2, MT1-MMP, and LN 5 γ 2 are important in tumor invasion. In addition to the preferential expression in the invading tumor fronts found in various types of primary human cancers,[4,7,25] these three molecules interact with each other in promoting tumor cell invasion. It has been shown that MMP-2, MT1-MMP, and TIMP-2 form a complex on the cell surface, where MT1-MMP binds to and activates pro-MMP-2 by proteolysis.[5] Both MMP-2 and MT1-MMP also cleave LN 5 γ 2 within the γ 2 chain (155 kd) and generate proteolytic fragments, γ 2′ (110 kd) and γ 2′ X (80 kd). The released γ 2′ X fragment is capable of promoting tumor cell invasion[8,9] and preventing tumor

Figure 3. Co-overexpression and co-activation of MT1-MMP and LN 5 γ 2 in the invasive edge of primary human glioma specimens. **A:** An example of performing microdissection on the center region (**a**, **circled area 1**) and invasive edge of the tumor (**a**, **circled area 2**). **a:** An overview of the specimen (J151, GBM, grade IV). **b** and **c:** Photographs of the central areas (**1** in **a**) and invasive edge (**2** in **a**) before microdissection. **d** and **e:** Photographs of the central areas (**1** in **a**) and invasive edge (**2** in **a**) after microdissection. **b** and **c:** Enlarged photos of tumor center (**circled area 1** in **a**). **c** and **e:** Tumor invasive edge (**circled area 2** in **a**). **B:** Western blot analyses of total protein extracted from microdissected glioma tissues of tumor center (**C**, illustrated as area **1** in **A**; **a**, **b**, and **d**) and tumor invasive edge (**B**, illustrated as area **2** in **A**; **a**, **c**, and **e**). OD grade II, specimen J181, an oligodendroastrocytoma; AA, grade III, specimen J165, an astrocytic astrocytoma; and J151, J152, and J155, GBM, grade IV, GBM. **Top**: Expression and activation of LN 5 γ 2; **middle**: expression and activation of MT1-MMP (the second panel), and **bottom**: β-actin (a loading control). Mature LN 5 γ 2 runs at 155 kd and cleaved γ2′ and γ2x run at 105 kd and 80 kd, respectively. Mature and autocleaved MT1-MMP run at 68 kd and 45 kd, respectively. β-Actin runs at 43 kd. The experiments were performed two independent times and similar results were obtained. Original magnifications: ×12.5 (**Aa**); ×40 (**Ab–Ae**).

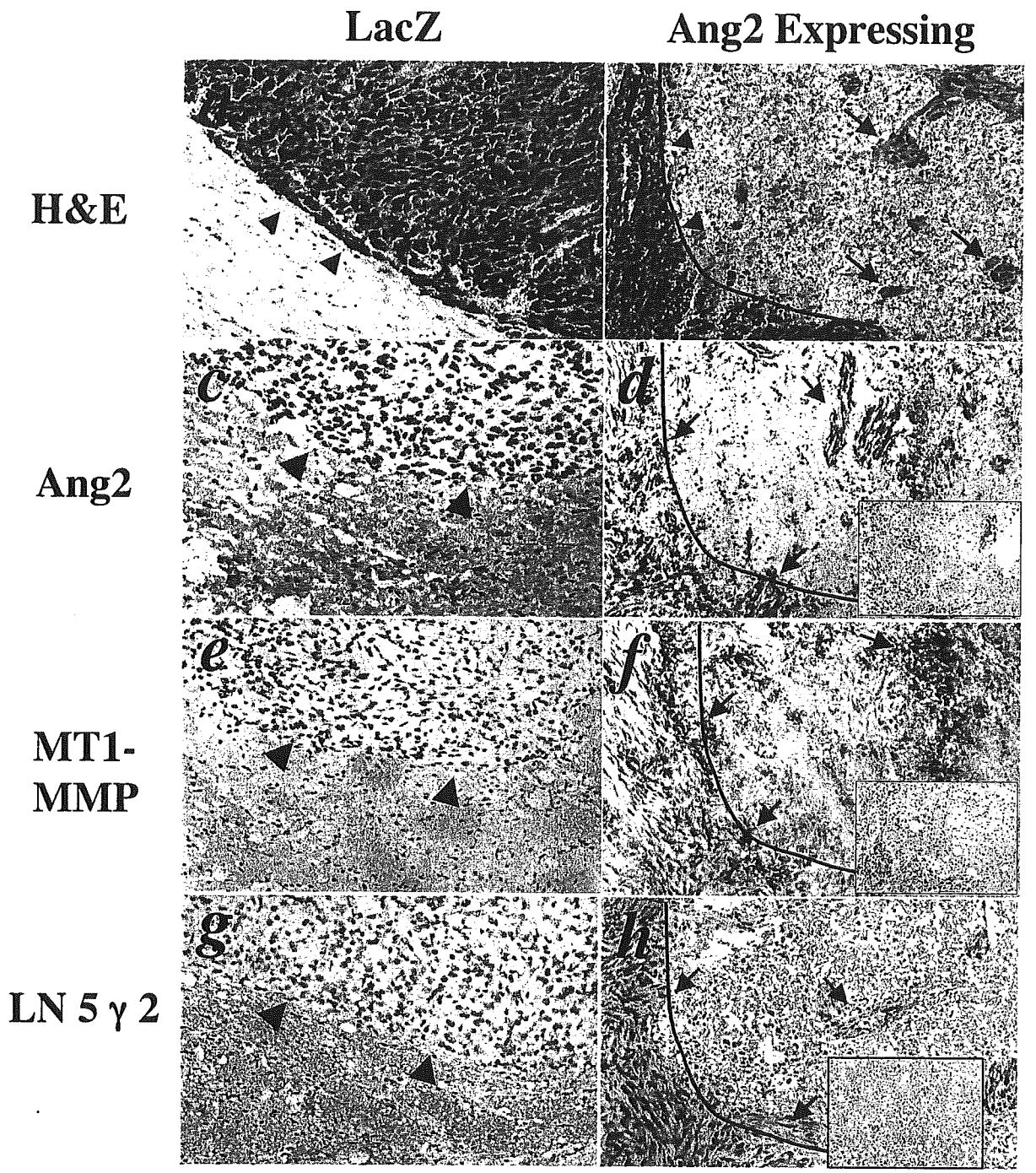

Figure 4. Overexpression of Ang2 by U87MG cells induces glioma invasion and promotes the expression of MT1-MMP and LN 5 γ 2 in the murine brain. IHC of various U87MG gliomas established in the murine brain. **a** to **d** were previously published in Hu and colleagues.[17] The only purpose that we present here again is to serve as controls showing that co-overexpression of Ang2, MT1-MMP, and LN 5 γ 2 are localized in the same invading glioma cells in the brain. **a**, **c**, **e**, and **g:** A glioma established by control U87MG/LacZ cells. **b**, **d**, **f**, and **h:** An invasive glioma formed by U87MG/Ang2 cells. **a** and **b:** H&E staining. **Arrowheads** in **a** indicate the clean edge of U87MG/LacZ tumor spheroid. **Arrowheads** in **b** indicate spikes extended from tumor mass of the U87MG/Ang2 glioma. **Arrows** in **b** show disseminated tumor clusters of U87MG/Ang2 gliomas. **c** to **h:** IHC on serial sections of U87MG/LacZ or U87MG/Ang2 gliomas using anti-Ang2 (**c**, **d**), anti-MT1-MMP (**e**, **f**), and anti-LN 5 γ 2 (**g**, **h**) antibodies. **Arrowheads** in **c**, **e**, and **g** indicate the clean edges of U87MG/LacZ tumor spheroid. **Arrows** in **d**, **f**, and **h** show the invasive tumor-spike and disseminated tumor clusters that expressed Ang2 (**d**), MT1-MMP (**f**), or LN 5 γ 2 (**h**). **Insets** in **d**, **f**, and **h** show isotype-matched IgG controls. Ten to twelve individual samples in each class were analyzed. The experiments were repeated two additional times with similar results. Original magnifications, ×200.

cell apoptosis through the interaction with the epidermal growth factor receptor.[27] LN 5 γ 2 and MT1-MMP are found to be co-localized in invasive fronts of human breast cancers.[9] Indeed, cooperative interactions of LN 5 γ 2, MMP-2, and MT1-MMP are required for tumor vascular mimicry vasculogenesis.[28,29] Our results corroborate these observations. We found that up-regulated expression of MMP-2, MT1-MMP, and LN 5 γ 2, but not

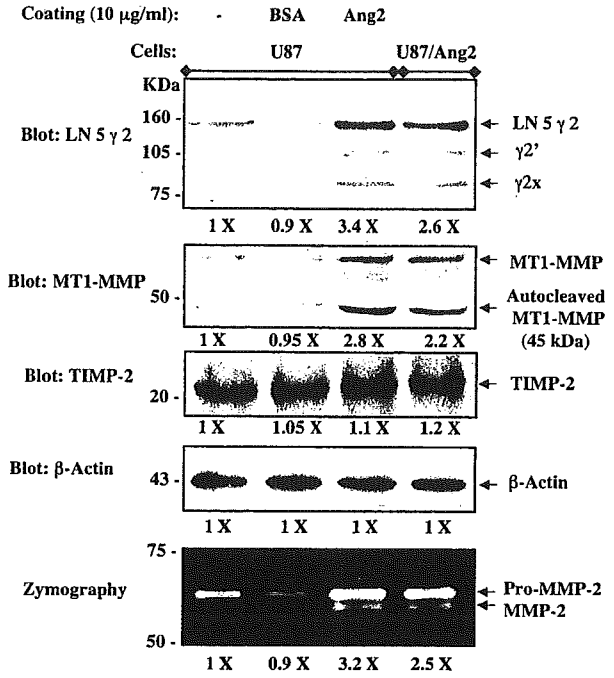

Figure 5. Stimulation of human glioma cells by overexpressing Ang2 or exogenous Ang2 promotes the expression and activation of MMP-2, MT1-MMP, and LN 5 γ 2, but not TIMP-2 *in vitro*. **Top** four panels: Western blot analyses for expression and activation of LN 5 γ 2 (the first panel from the **top**), MT1-MMP (the second panel), TIMP-2 (the third panel), and β-actin (the fourth panel, a loading control). Mature LN 5 γ 2 runs at 155 kd and cleaved γ2' and γ2x run at 105 kd and 80 kd, respectively. Mature and autocleaved MT1-MMP run at 68 kd and 45 kd, respectively. TIMP-2 runs at 22 kd. β-Actin runs at 43 kd. **Bottom**: Zymography assays for the activation of MMP-2. The pro-MMP-2 and the mature form of MMP-2 are shown at 72 kd and 64 kd, respectively.

TIMP-2, co-localized with the increased Ang2 in the invasive areas of primary human glioma specimens, in U87MG Ang2-expressing gliomas *in vivo* as well as in Ang2-stimulated glioma cells *in vitro*. Interestingly, stronger proteolytic co-activation of LN 5 γ 2 and MT1-MMP were found in the proteins extracts from microdissected primary glioma invasive tissues (Figure 3B) than the Ang2 stimulation (by overexpression or exogenous treatment with recombinant Ang2) of U87MG glioma cells *in vitro*, suggesting an optimal tumor microenvironment *in vivo* was more potent in stimulating the activities of these two extracellular matrix-modifying enzymes critical for glioma cell invasion. Thus, our data indicate that co-overexpression of these molecules is involved in glioma invasion.

The ability of glioma cells to diffusively infiltrate normal brain tissues without disrupting brain cytoarchitecture or neuronal function is a hallmark of malignant human gliomas.[1–3] Glioma invasion does not correlate with glioma grade because low-grade astrocytomas invade brain parenchyma with high frequency. However, the degree of tumor invasiveness is correlated with glioma grade.[1–3] In this study, seven of eight PAs displayed an infiltrative phenotype (Table 1) whereas grade II III, and IV glioma specimens in our collection contain distinct invasiveness with identifiable tumor border and invasive areas. Expression profiles of Ang2, MMP-2, MT1-MMP, and LN 5 γ 2 are correlated with the invasive edge of human gliomas, especially in the invasive areas that are 0.25 mm away from the tumor border. Increased levels of these proteins were evident in the invasive regions in these grade I to IV tumors (Tables 1 and 2; Figures 2A, 2B, and 2C, f, i, l, o; and data not shown) and in the tumor borders (Tables 1 and 2; Figures 2A, 2B, and 2C, e, h, k, n; and data not shown). When compared with the other three molecules, the expression profiles of LN 5 γ 2 were relatively increased in both invasive and noninvasive regions of grade IV GBM tumors (Table 1). Strong activation of LN 5 γ 2 at the invasive edge of the tumor (Figure 3B) supports our IHC data that this tumor invasion marker is involved in the progressive growth of malignant GBM tumors. These data show that up-regulation of these four molecules, particularly Ang2, MMP-2, and MT1-MMP, is correlated with the invasiveness of malignant human gliomas.

In summary, our data demonstrate that co-localization of up-regulated Ang2, MMP-2, MT1-MMP, and LN 5 γ 2 is significantly associated with human glioma invasion. Our results from the engineered human U87MG glioma (Ang2-overexpressing, Figure 4) xenografts and cell culture model (stimulation of glioma cells by overexpressing Ang2 or exposure to exogenous Ang2, Figure 5), and from previous reports[30–33] suggest that Ang2 plays a critical role in promoting human glioma invasion through the activation of MMP-2, MT1-MMP, and LN 5 γ 2 in Tie2-independent-pathways. The determination of the mechanisms by which Ang2 induces glioma invasion could provide critical information with regard to the potential of Ang2 and its effectors as new therapeutic targets in glioma treatments.

Acknowledgments

We thank Dr. R. Hamilton for his help in identification of WHO glioma grades and tumor invasiveness in primary human glioma specimens, Dr. Jennifer Hunt and Deren M. Lomago for their help in microdissection of paraffin-embedded primary human glioma specimens, and Christopher A. Schafer for his technical assistance in the IHC staining.

References

1. Giese A, Westphal M: Glioma invasion in the central nervous system. Neurosurgery 1996, 39:232–250
2. Berger MS, Wilson CB: The Gliomas. Philadelphia, W.B. Saunders Company, 1999
3. Kleihues P, Cavenee WK (eds): Pathology and Genetics: Tumours of the Nervous System. Lyon, IARC Press, 2000
4. Brinckerhoff CE, Matrisian LM: Matrix metalloproteinases: a tail of a frog that became a prince. Nat Rev Mol Cell Biol 2002, 3:207–214
5. Sternlicht MD, Werb Z: How matrix metalloproteinases regulate cell behavior. Annu Rev Cell Dev Biol 2001, 17:463–516
6. Kleiner DE, Stetler-Stevenson WG: Matrix metalloproteinases and metastasis. Cancer Chemother Pharmacol 1999, 43:S42–S51
7. Lohi J: Laminin-5 in the progression of carcinomas. Int J Cancer 2001, 94:763–767
8. Giannelli G, Falk-Marzillier J, Schiraldi O, Stetler-Stevenson WG, Quaranta V: Induction of cell migration by matrix metalloprotease-2 cleavage of laminin-5. Science 1997, 277:225–228
9. Koshikawa N, Giannelli G, Cirulli V, Miyazaki K, Quaranta V: Role of cell surface metalloprotease MT1-MMP in epithelial cell migration over laminin-5. J Cell Biol 2000, 148:615–624

10. Yancopoulos GD, Davis S, Gale NW, Rudge JS, Wiegand SJ, Holash J: Vascular-specific growth factors and blood vessel formation. Nature 2000, 407:242–248
11. Ahmad SA, Liu W, Jung YD, Fan F, Wilson M, Reinmuth N, Shaheen RM, Bucana CD, Ellis LM: The effects of angiopoietin-1 and -2 on tumor growth and angiogenesis in human colon cancer. Cancer Res 2001, 61:1255–1259
12. Etoh T, Inoue H, Tanaka S, Barnard GF, Kitano S, Mori M: Angiopoietin-2 is related to tumor angiogenesis in gastric carcinoma: possible in vivo regulation via induction of proteases. Cancer Res 2001, 61: 2145–2153
13. Ogawa M, Yamamoto H, Nagano H, Miyake Y, Sugita Y, Hata T, Kim BN, Ngan CY, Damdinsuren B, Ikenaga M, Ikeda M, Ohue M, Nakamori S, Sekimoto M, Sakon M, Matsuura N, Monden M: Hepatic expression of ANG2 RNA in metastatic colorectal cancer. Hepatology 2004, 39:528–539
14. Ochiumi T, Tanaka S, Oka S, Hiyama T, Ito M, Kitadai Y, Haruma K, Chayama K: Clinical significance of angiopoietin-2 expression at the deepest invasive tumor site of advanced colorectal carcinoma. Int J Oncol 2004, 24:539–547
15. Sfiligoi C, de Luca A, Cascone I, Sorbello V, Fuso L, Ponzone R, Biglia N, Audero E, Arisio R, Bussolino F, Sismondi P, De Bortoli M: Angiopoietin-2 expression in breast cancer correlates with lymph node invasion and short survival. Int J Cancer 2003, 103:466–474
16. Ahmad SA, Liu W, Jung YD, Fan F, Reinmuth N, Bucana CD, Ellis LM: Differential expression of angiopoietin-1 and angiopoietin-2 in colon carcinoma. A possible mechanism for the initiation of angiogenesis. Cancer 2001, 92:1138–1143
17. Hu B, Guo P, Fang Q, Tao HQ, Wang D, Nagane M, Huang HJ, Gunji Y, Nishikawa R, Alitalo K, Cavenee WK, Cheng SY: Angiopoietin-2 induces human glioma invasion through the activation of matrix metalloprotease-2. Proc Natl Acad Sci USA 2003, 100:8904–8909
18. Guo P, Xu L, Pan S, Brekken RA, Yang ST, Whitaker GB, Nagane M, Thorpe PE, Rosenbaum JS, Su Huang HJ, Cavenee WK, Cheng SY: Vascular endothelial growth factor isoforms display distinct activities in promoting tumor angiogenesis at different anatomic sites. Cancer Res 2001, 61:8569–8577
19. Guo P, Hu B, Gu W, Xu L, Wang D, Huang HJ, Cavenee WK, Cheng SY: Platelet-derived growth factor-B enhances glioma angiogenesis by stimulating vascular endothelial growth factor expression in tumor endothelia and by promoting pericyte recruitment. Am J Pathol 2003, 162:1083–1093
20. Rolston R, Sasatomi E, Hunt J, Swalsky PA, Finkelstein SD: Distinguishing de novo second cancer formation from tumor recurrence: mutational fingerprinting by microdissection genotyping. J Mol Diagn 2001, 3:129–132
21. Ikeda K, Monden T, Kanoh T, Tsujie M, Izawa H, Haba A, Ohnishi T, Sekimoto M, Tomita N, Shiozaki H, Monden M: Extraction and analysis of diagnostically useful proteins from formalin-fixed, paraffin-embedded tissue sections. J Histochem Cytochem 1998, 46:397–403
22. Martinet W, Abbeloos V, Van Acker N, De Meyer GR, Herman AG, Kockx MM: Western blot analysis of a limited number of cells: a valuable adjunct to proteome analysis of paraffin wax-embedded, alcohol-fixed tissue after laser capture microdissection. J Pathol 2004, 202:382–388
23. Hofmann UB, Westphal JR, Zendman AJ, Becker JC, Ruiter DJ, van Muijen GN: Expression and activation of matrix metalloproteinase-2 (MMP-2) and its co-localization with membrane-type 1 matrix metalloproteinase (MT1-MMP) correlate with melanoma progression. J Pathol 2000, 191:245–256
24. Maher EA, Furnari FB, Bachoo RM, Rowitch DH, Louis DN, Cavenee WK, DePinho RA: Malignant glioma: genetics and biology of a grave matter. Genes Dev 2001, 15:1311–1333
25. Seiki M: Membrane-type 1 matrix metalloproteinase: a key enzyme for tumor invasion. Cancer Lett 2003, 194:1–11
26. Koga K, Todaka T, Morioka M, Hamada J, Kai Y, Yano S, Okamura A, Takakura N, Suda T, Ushio Y: Expression of angiopoietin-2 in human glioma cells and its role for angiogenesis. Cancer Res 2001, 61: 6248–6254
27. Schenk S, Hintermann E, Bilban M, Koshikawa N, Hojilla C, Khokha R, Quaranta V: Binding to EGF receptor of a laminin-5 EGF-like fragment liberated during MMP-dependent mammary gland involution. J Cell Biol 2003, 161:197–209
28. Seftor RE, Seftor EA, Koshikawa N, Meltzer PS, Gardner LM, Bilban M, Stetler-Stevenson WG, Quaranta V, Hendrix MJ: Cooperative interactions of laminin 5 gamma2 chain, matrix metalloproteinase-2, and membrane type-1-matrix/metalloproteinase are required for mimicry of embryonic vasculogenesis by aggressive melanoma. Cancer Res 2001, 61:6322–6327
29. Hess AR, Seftor EA, Seftor RE, Hendrix MJ: Phosphoinositide 3-kinase regulates membrane Type 1-matrix metalloproteinase (MMP) and MMP-2 activity during melanoma cell vasculogenic mimicry. Cancer Res 2003, 63:4757–4762
30. Fukushima Y, Ohnishi T, Arita N, Hayakawa T, Sekiguchi K: Integrin alpha3beta1-mediated interaction with laminin-5 stimulates adhesion, migration and invasion of malignant glioma cells. Int J Cancer 1998, 76:63–72
31. Chintala SK, Sawaya R, Gokaslan ZL, Rao JS: Modulation of matrix metalloprotease-2 and invasion in human glioma cells by alpha 3 beta 1 integrin. Cancer Lett 1996, 103:201–208
32. Knott JC, Mahesparan R, Garcia-Cabrera I, Bolge Tysnes B, Edvardsen K, Ness GO, Mork S, Lund-Johansen M, Bjerkvig R: Stimulation of extracellular matrix components in the normal brain by invading glioma cells. Int J Cancer 1998, 75:864–872
33. Giannelli G, Bergamini C, Fransvea E, Marinosci F, Quaranta V, Antonaci S: Human hepatocellular carcinoma (HCC) cells require both alpha3beta1 integrin and matrix metalloproteinases activity for migration and invasion. Lab Invest 2001, 81:613–627

Available online at www.sciencedirect.com

SCIENCE DIRECT

Surgical Neurology 63 (2005) 375–379

SURGICAL NEUROLOGY

www.surgicalneurology-online.com

Mixed neuronal-glial tumor of the fourth ventricle and successful treatment of postoperative mutism with bromocriptine: case report

Jun-ichi Adachi, MD[a,*], Ryo Nishikawa, MD[a], Takanori Hirose, MD[b], Masao Matsutani, MD[a]

Departments of [a]Neurosurgery, and [b]Pathology, Saitama Medical School, Saitama 350-0495, Japan

Received 10 March 2004; accepted 10 May 2004

Abstract

Background: Tumors composed of both neurocytic and astrocytic cells are uncommon and poorly understood. We describe the clinicopathologic features of a very rare rosette-forming glioneuronal tumor of the fourth ventricle and propose bromocriptine as a useful therapeutic agent for cerebellar mutism after posterior fossa surgery.

Case Description: A fourth ventricle tumor was incidentally discovered in an 18-year-old woman. Magnetic resonance imaging revealed ventriculomegaly and a solid tumor with low-intensity signals on T1-weighted images and high-intensity signals on T2-weighted images. There was slight gadolinium enhancement. The tumor was subtotally resected. Although its lower half was well circumscribed, its upper half manifested invasive growth. Histologically, 2 components were identified, synaptophysin-positive neurocytic cells forming perivascular pseudorosettes and glial fibrillary acidic protein–positive astrocytic cells with Rosenthal fibers. Overall, cellular atypia was minimal and the MIB-1 labeling index was low. On the basis of these histologic findings, the tumor bore striking similarity to the recently described rosette-forming glioneuronal tumors of the fourth ventricle. Postoperatively, the patient manifested cerebellar mutism. The administration of bromocriptine improved her neurological status dramatically.

Conclusion: The natural history of rosette-forming glioneuronal tumors of the fourth ventricle is not yet fully understood. Therefore, careful and long-term follow-up monitoring of the tumor hosts is necessary. Bromocriptine therapy may promote recovery from mutism after posterior fossa surgery.

Keywords: Glioneuronal tumor; Fourth ventricle; Bromocriptine

1. Introduction

Although in the World Health Organization (WHO) classification of central nervous system tumors [12] some neoplasms are differentiated along neuronal and glial lines, their clinicopathologic features remain to be fully elucidated. We now present a patient with a rare mixed neuronal-glial tumor of the fourth ventricle.

2. Case report

The patient was an 18-year-old woman who was involved in a traffic accident in December 1999. On the basis of computed tomography (CT) scan and magnetic resonance imaging (MRI) obtained upon admission, a mass lesion in the fourth ventricle was incidentally detected. Her general condition was good and she was alert. She had a several-year history of occasional headache. Careful neurologic examination revealed slight cerebellar truncal ataxia. Laboratory examinations returned normal results.

Plain skull radiography disclosed diastasis of the cranial sutures and many digital markings, suggestive of chronic increased intracranial pressure. Magnetic resonance imaging demonstrated a tumor, measuring approximately 3.0 cm in diameter, occupying the fourth ventricle; there was associated ventriculomegaly. The tumor manifested as a low- and high-intensity solid mass on T1- and T2-weighted magnetic resonance images, respectively (Fig. 1A and B). The lesion seemed relatively well demarcated; it extended into the

* Corresponding author. Tel.: +81 49 276 1334; fax: +81 49 294 4955.
E-mail address: jadachi@saitama-med.ac.jp (J. Adachi).

0090-3019/$ – see front matter © 2005 Elsevier Inc. All rights reserved.
doi:10.1016/j.surneu.2004.05.039

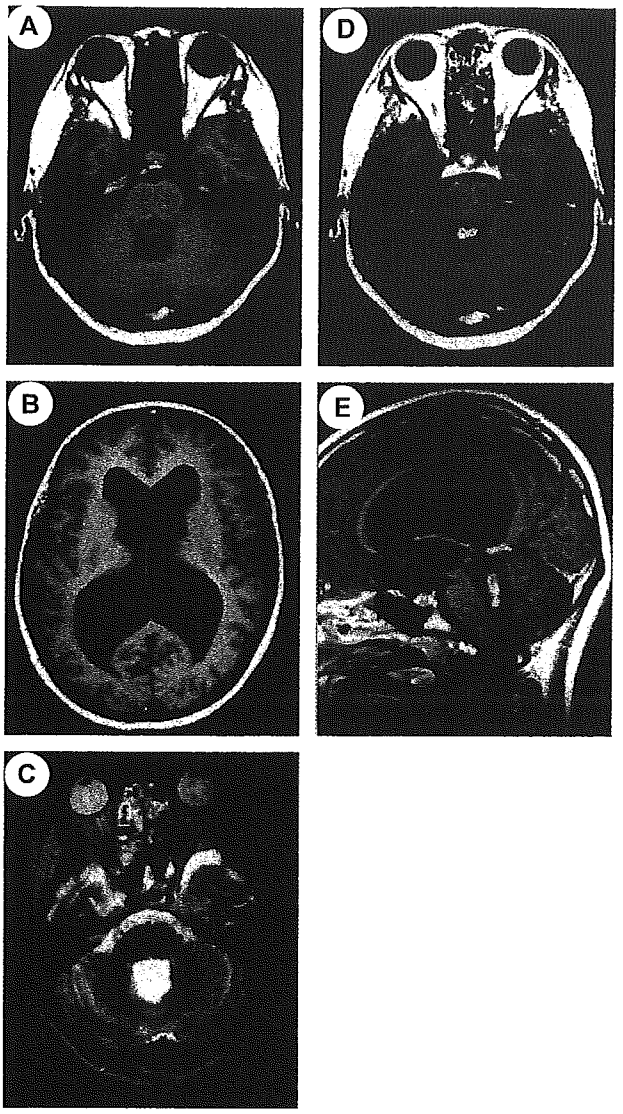

Fig. 1. Magnetic resonance imaging scans on admission. A and B: Axial T1-weighted MRI showing a low-intensity mass in the fourth ventricle and enlargement of the lateral ventricles. C: Axial T2-weighted MRI visualizing the mass as an area of high intensity. D and E: Axial (D) and sagittal (E) T1-weighted MRI scans obtained after the injection of gadolinium-diethylenetriamine pentaacetic acid show enhancement of the center portion of the mass.

aqueduct and compressed the superior vermis posteriorly without significant peritumoral edema. After the intravenous injection of gadolinium-diethylenetriamine pentaacetic acid, the center portion of the tumor exhibited slight enhancement on T1-weighted magnetic resonance images (Fig. 1C and D). Bilateral vertebral angiograms revealed no tumor stain.

Since the patient did not develop definite symptoms of increased intracranial pressure, we did not use ventricular drain preoperatively. With the patient in the prone position, suboccipital craniotomy was performed through a midline scalp incision. Lateral retraction of the cerebellar tonsils exposed a grayish solid tumor of soft consistency. The lower half of the tumor was well circumscribed with no macroscopic invasion into adjacent structures. However, its upper half exhibited invasive growth and there was no clear deliniation between the tumor and the surrounding cerebellar parenchyma. The tumor was subtotally removed with a small portion remaining in the upper vermis.

Histological examination of the surgical specimen demonstrated that the tumor was composed of neuronal and glial components (Fig. 2A). The neuronal component

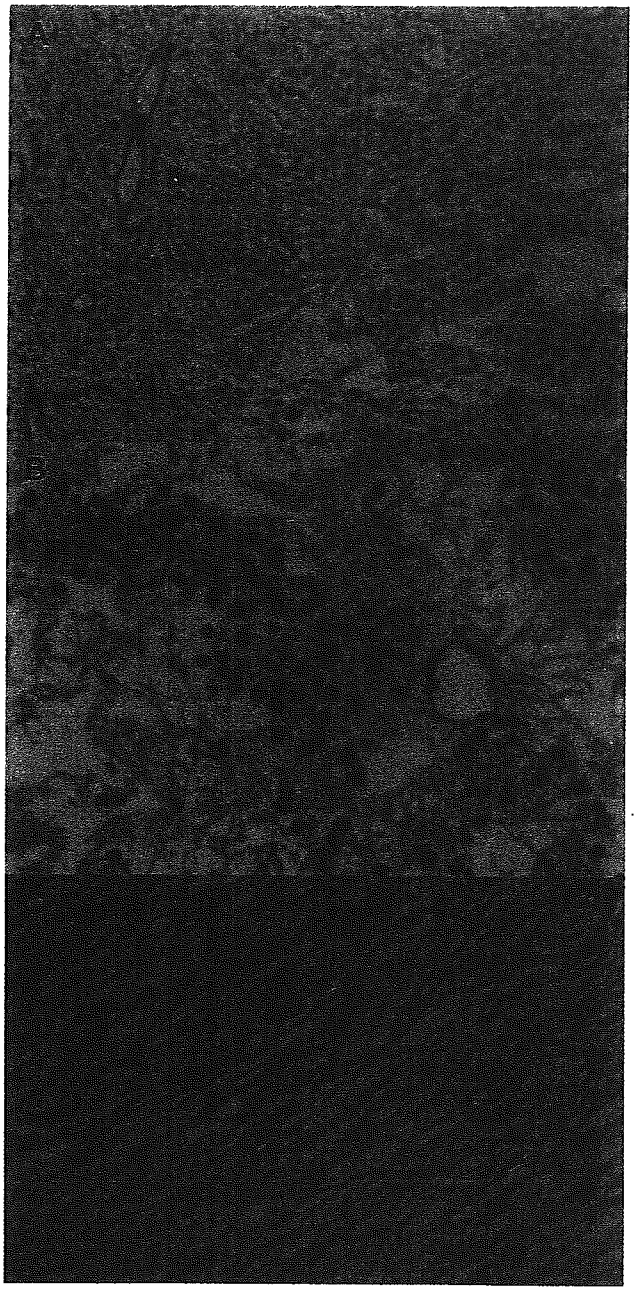

Fig. 2. Photomicrographs of the tumor specimen showing a mixed neuronal-glial tumor. A: Overview of the two major components, one neuronal (right), the other glial (left) (hematoxylin and eosin, original magnification 200×). B: Higher magnification of neurocytes and perivascular pseudorosette formation (hematoxylin and eosin, original magnification 400×). C: Higher magnification of the dense fibrillated area identical to pilocytic astrocytoma. Note the Rosenthal fibers (arrow) (hematoxylin and eosin, original magnification 400×).

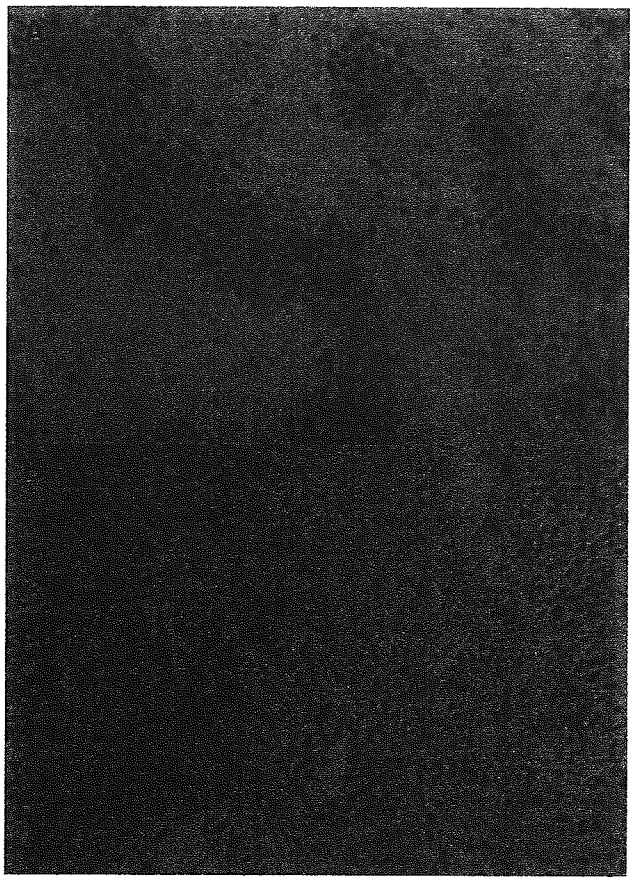

Fig. 3. Immunohistochemical analysis. A: Strong positivity for synaptophysin at the area of the perivascular pseudorosette (original magnification 200×). B: Glial fibrillary acidic protein expression is restricted to the compact glial component (left) (original magnification 200×).

consisted of uniform neurocytic cells in a fibrillary, partly microcystic matrix with perivascular pseudorosette formation (Fig. 2B). The glial component consisted of fibrillated, spindle astrocytic cells with oval nuclei in a dense fibrillary background. These cells were aggregates of neoplastic astrocytes; they were not reactive. There were occasional Rosenthal fibers and granular bodies; thus, the glial component most resembled pilocytic astrocytoma (Fig. 2C). In proportion, the 2 components were almost equal. There were no evident mitoses, necrotic areas, or vascular proliferation. Immunohistochemical studies showed that the center of the neurocytic cells and the perivascular pseudorosettes were immunoreactive for synaptophysin (Fig. 3A). Glial fibrillary acidic protein expression was strongly positive in the pilocytic portions of the glial component but absent in the neurocytic component (Fig. 3B). The proliferative index, assessed by MIB-1 immunostaining of tumor cell nuclei, was less than 1% in both components. Ultrastructurally, the neurocytic cells were characterized by round nuclei and scant cytoplasm containing undeveloped rough endoplasmic reticulum and prominent Golgi apparatus. Occasional cytoplasmic processes contained sparse, dense core granules. Mature synaptic terminals were frequently seen to contact the cell bodies (Fig. 4). On the other hand, astrocytic cells manifested heterochromatic nuclei and cytoplasm containing dense bundles of glial filaments. On the basis of these histological, immunohistochemical, and ultrastructural findings, this case was diagnosed as a mixed neuronal-glial tumor showing both neuronal and glial differentiation.

For the first 8 postoperative days, the patient was in a slightly somnolent state; she was able to communicate verbally. However, her consciousness gradually deteriorated, and after the 14th postoperative day she was barely able to respond to verbal or pain stimuli. There were few movements, her oral communication was markedly reduced, and she lapsed into an almost comatose state. Laboratory examination revealed no abnormalities related to her consciousness deterioration. Magnetic resonance imaging demonstrated decreased ventricular size; on T2-weighted MRI there was no evident damage to the brainstem. No perifocal edema was noted. Lumbar puncture, performed on the 14th postoperative day to measure the cerebrospinal fluid pressure, revealed that the initial pressure was within normal limits. Radioisotope cisternography demonstrated the normal pattern of cerebrospinal fluid dynamics. Therefore, we rejected shunt placement. Brain single-photon emission CT with technetium ^{99m}Tc ethyl cysteinate dimer revealed reduced perfusion in the bilateral frontal lobes and right thalamus. Although therapy with corticosteroids and thyrotropin-releasing hormone was administered, she failed to manifest clinical improvement.

Starting on the 37th postoperative day, we began bromocriptine therapy at a dose of 3 × 2.5 mg/day through a nasogastric tube; 24 hours later she began to open her eyes to pain. From the next day, the bromocriptine dose was increased to 3 × 5.0 mg and maintained. Two days later her eye-open time increased and she started to speak and to spontaneously move her extremities. Over the next 2 weeks, she returned to almost complete alertness and showed

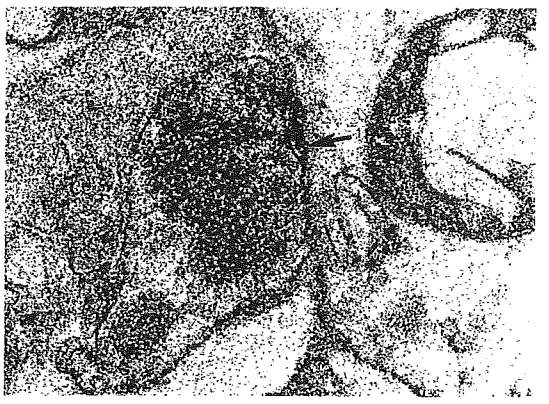

Fig. 4. Ultrastructural analysis of the neurocytic cells. Note the occasional synaptic contacts (arrow) containing clear vesicles on the cell bodies (original magnification 20000×).

marked recovery, including eating without assistance and speaking more fluently. On the 127th postoperative day, she was discharged on bromocriptine at a dose of 15.0 mg/day. During a 4-year follow-up, she has remained well except for mild cerebellar truncal ataxia. There have been no signs of tumor recurrence on follow-up MRI.

3. Discussion

We posit that the neoplasm in our case is like the rosette-forming glioneuronal tumor of the fourth ventricle reported by Komori et al [13] in 1998 who included it in their later series of "rosette-forming glioneuronal tumor of the fourth ventricle" [14]. This variant of mixed glioneuronal tumors involves primarily the fourth ventricle and consists of well-differentiated neurocytes and pilocytic astrocytes. Analysis of 11 rosette-forming glioneuronal tumors indicated that the age of patients ranged from 12 to 59 years (mean, 31.5 years); male-female ratio was 1:1.75 [14]. The most common symptom was headache lasting from months to years. Neurologically, cerebellar ataxia was observed in more than half of their cases; only one patient manifested brainstem impairment. All tumors were located in the midline and occupied the fourth ventricle with moderate to marked hydrocephalus. Magnetic resonance imaging typically showed a well-circumscribed solid mass. Cystic components were noted in 9 of their 11 cases, and peritumoral edema was minimal. Contrast enhancement, while typical, was only focal and curvilinear, ringlike, or spotlike. Macroscopically, the tumors were soft and the intraventricular tumor portions were usually resectable. However, tumor tissue infiltrating the surrounding brain parenchyma was often left. Lack of atypia, low MIB-1 labeling indices, and their indolent clinical course suggest that these tumors are of a low-grade (WHO I) status.

The tumor we encountered here was a glioneuronal tumor exhibiting all of the above-mentioned features. Its neuronal differentiation was even more striking because our ultrastructural study revealed mature synaptic terminals on the surface of neurocytic cells.

From the perspective of a prominent "glioneuronal" appearance, the histological differential diagnosis in our patient included dysembryoplastic neuroepithelial tumor (DNT) and ganglioglioma. DNTs are benign neoplasms characterized by their occurrence in children and adolescents [7,11]. They are usually located in the supratentorial cortex and include a long history of partial seizures [7]. Most gangliogliomas are supratentorial and preferentially involve the temporal lobe [10,15,19]. Our case, however, lacked these features. Above all, the presence of rosette formation, indicative of a differentiated neuronal phenotype, made our case inconsistent with a diagnosis of DNT or ganglioglioma.

Rosette-forming glioneuronal tumors of the fourth ventricle contain both glial and neuronal elements [13,14]. It remains unknown whether they arise from a single neoplastic precursor cell giving rise to glial and neuronal cell types because of divergent differentiation, or from independent glial and neuronal cells within the same tumor. Molecular analysis of their clonal derivation will provide important evidence about the underlying tumorigenesis, as it did in clonality assay of gangliogliomas [20]. Interestingly, this type of mixed glioneuronal tumor arises preferentially in the fourth ventricle.

Postoperatively, our patient manifested severe consciousness disturbance reminiscent of akinetic mutism, which is most often seen in patients with obstructive hydrocephalus, bilateral brain damage to the anterior cingulate gyri, mesencephalic-diencephalic reticular formation, and basal ganglia [3,4,6,16,18]. However, her hydrocephalus was improved on postoperative MRI and the location of the tumor was infratentorial. On the other hand, cerebellar mutism sometimes occurs after surgery to posterior fossa tumors, especially surgery involving the removal of large midline tumors [8]. Our case may represent an extreme case of this syndrome. The destruction of the mesencephalon or the cerebellar substance involving the deep nuclei is probably the most important anatomical substrate of mutism [17]. In addition to direct parenchymal damage, vasospasm of one or more vessels supplying relevant areas contributes to the onset of cerebellar mutism. Ferrante et al [8] noted that, as in our case, there was a postoperative period during which their patients were in good neurological condition. The 3 major monoaminergic pathways consisting of dopaminergic, noradrenergic, and serotonergic projections originate in the mesencephalon [1,2,17]. The dopaminergic projection regulating voluntary movements and cognition runs through the medial forebrain bundles of the far-lateral hypothalamus and terminates in the striatum or the frontal cortex.

According to our clinical and neuroradiological evidence, the dopaminergic pathway was most probably involved in the akinetic mutism observed in our case. First, the patient drastically improved on bromocriptine. Bromocriptine binds to D_2 dopamine receptors and increases dopamine level [9]. If her akinetic mutism was attributed to damage of restricted lesion of the dopamine pathways, she was expected to recover by the administration of bromocriptine. She immediately responded to bromocriptine and manifested clinical improvement dramatically within 2 weeks. For ethical reasons, we did not take our patient off bromocriptine to observe whether she would relapse into a comatose state. Caner et al [5] reported that a patient with akinetic mutism after the removal of a fourth ventricle tumor was successfully treated with bromocriptine. Second, on postoperative single-photon emission CT we noted bilateral frontal ischemia; we attributed this to diaschisis due to injury of the mesencephalon monoaminergic system [5]. On the basis of our observations we suggest that bromocriptine therapy may be efficacious in patients who manifest mutism after posterior fossa surgery.

Because the tumor reported here manifested minimal cytologic atypia and a low MIB-1 labeling index, we diagnosed it as a low-grade malignancy. In the series of Komari et al [14], none of the 11 rosette-forming glioneuronal tumors recurred postoperatively. As was true in our patient, in 6 of their cases, the tumors showed infiltrative growth into adjacent tissue. Careful, long-term follow-up monitoring is necessary to assess the biological behavior of these tumors. As cerebellar mutism is a difficult complication after posterior fossa surgery, we wish to stress the potent effect of bromocriptine therapy noted in our patient.

Acknowledgments

The authors thank Noriko Murai for her excellent technical assistance in the ultrastructural study and Ursula Petralia for editorial assistance.

References

[1] Anderson B. Relief of akinetic mutism from obstructive hydrocephalus using bromocriptine and ephedrine. J Neurosurg 1992;76:152-5.
[2] Barrett K. Treating organic abulia with bromocriptine and lisuride: four case studies. J Neurol Neurosurg Psychiatry 1991;54:718-21.
[3] Berger L, Gauthier S, Leblanc R. Akinetic mutism and parkinsonism associated with obstructive hydrocephalus. Can J Neurol Sci 1985;12: 255-8.
[4] Cairns H, Oldfield RC, Pennybacker JB, et al. Akinetic mutism with an epidermoid cyst of the third ventricle. Brain 1941;64:273-90.
[5] Caner H, Altinors N, Benli S, et al. Akinetic mutism after fourth ventricle choroid plexus papilloma: treatment with a dopamine agonist. Surg Neurol 1999;51:181-4.
[6] Cravioto D, Silberman J, Feigi I. A clinical and pathological study of akinetic mutism. Neurol Minneapolis 1960;10:10-21.
[7] Daumas-Duport C, Scheithauer BW, Chodkiewicz JP, et al. Dysembryoplastic neuroepithelial tumor: a surgically curable tumor of young patients with intractable partial seizures. Reports of thirty-nine cases. Neurosurgery 1988;23:545-56.
[8] Ferrante L, Mastronardi L, Acui M, et al. Mutism after posterior fossa surgery in children. Report of three cases. J Neurosurg 1990;72:959-63.
[9] Fluckiger E, Kovacs E. Inhibition by 2-ergokryptine-mesylate (CB154) of suckling-induced pituitary prolactin depletion in lactating rats. Experientia 1974;30:1173.
[10] Hirose T, Scheithaue BW, Lopes MBS, et al. Ganglioglioma: an ultrastructural and immunohistochemical study. Cancer 1997;9: 989-1003.
[11] Honavar M, Janota I, Polkey CE. Histological heterogeneity of dysembryoplastic neuroepithelial tumour: identification and differential diagnosis in a series of 74 cases. Histopathology 1999;34:342-56.
[12] Kleihues P, Cavenee WK. Pathology and genetics of tumours of the nervous system. Lyon: IARC Press; 2000.
[13] Komori T, Scheithauer BW, Sung J. Rosette-forming mixed neuronal-glial tumor in the fourth ventricle. J Neuropathol Exp Neurol 1988;57: 520 [Abstract].
[14] Komori T, Scheithauer BW, Hirose T. A rosette-forming glioneuronal tumor of the fourth ventricle: infratentorial form of dysembryoplastic neuroepithelial tumor? Am J Surg Pathol 2002;26:582-91.
[15] Lang FF, Epstein FJ, Ransohoff J, et al. Central nervous system gangliogliomas: Part 2. Clinical outcome. J Neurosurg 1993;79: 867-73.
[16] Nielsen JM, Jacobs LL. Bilateral lesions of the anterior cingulate gyri. Bull Los Angel Neurol Soc 1951;16:231-4.
[17] Role LW, Kelly JP. The brain stem. Cranial nerve nuclei and the monoaminergic systems. In: Kandel ER, Schwartz JH, editors. Principles of neural science. New York: Elsevier; 1981. p. 697-9.
[18] Rose ED, Stewart RM. Akinetic mutism from hypothalamic damage: successful treatment with dopamine agonists. Neurology 1981;31: 1435-9.
[19] Wolf HK, Muller MB, Spanle M, et al. Gangliogliomas: a detailed histopathological and immunohistochemical analysis of 61 cases. Acta Neuropathol (Berl) 1994;88:166-73.
[20] Zhu JJ, Leon SP, Folkerth RD, et al. Evidence for clonal origin of neoplastic neuronal and glial cells in gangliogliomas. Am J Pathol 1997;151:565-71.

Few men desire liberty; the majority are satisfied with a just master.

—Gaius Sallustius Crispus
(c. 86–35/45 B.C.), Roman historian. Histories, IV.